

**IMPACT OF EARTHING DEVIATION
ON SURGE PROTECTION DEVICES**

LEE YAO DONG

**A project report submitted in partial fulfilment of the
requirements for the award of Bachelor of Engineering
(Honours) Electrical and Electronic Engineering**

**Lee Kong Chian Faculty of Engineering and Science
Universiti Tunku Abdul Rahman**

January 2021

DECLARATION

I hereby declare that this project report is based on my original work except for citations and quotations which have been duly acknowledged. I also declare that it has not been previously and concurrently submitted for any other degree or award at UTAR or other institutions.

Signature : DONG

Name : LEE YAO DONG

ID No. : 1703221

Date : 19/04/2021

APPROVAL FOR SUBMISSION

I certify that this project report entitled “**IMPACT OF EARTHING DEVIATION ON SURGE PROTECTION DEVICES**” was prepared by **LEE YAO DONG** has met the required standard for submission in partial fulfilment of the requirements for the award of Bachelor of Engineering (Honours) Electrical and Electronic Engineering at Universiti Tunku Abdul Rahman.

Approved by,

Signature :



Supervisor :

Dr. Chew Kuew Wai

Date :

19/04/2021

Signature :

Co-Supervisor :

Date :

The copyright of this report belongs to the author under the terms of the copyright Act 1987 as qualified by Intellectual Property Policy of Universiti Tunku Abdul Rahman. Due acknowledgement shall always be made of the use of any material contained in, or derived from, this report.

© 2021, Lee Yao Dong. All right reserved.

ACKNOWLEDGEMENTS

I would like to thank Universiti Tunku Abdul Rahman for giving me this opportunity to perform research on this project. Dr. Chew Kuew Wai has been an invaluable supervisor in providing guidance and tremendous support in helping me making this research possible.

In addition, the utmost gratitude to Mr. Kuan Teik Hua of KL Automation Engineering Sdn. Bhd. in clarifying my doubts throughout the research process of this project.

ABSTRACT

Power surge is a phenomenon where a sudden rush of energy is being introduced into a system. Among many surges, lightning is the more common one that is familiar in the eyes of the public. Surges are destructive in nature and often times cause unnecessary damages to equipment or even human lives. A surge protection device (SPD) can be used as a protective equipment to prevent such unfortunate events to occur. In this research, the different sources of which surges originated from is explored while studies are performed to investigate how earth impedance can affect the performance of the SPD to react towards a surge event. In this project, a surge generator is modelled and is able to generate a desired surge waveform that is in accordance to the IEEE 6100-4-5 standard. Applying the surge onto an electrical network, it was found that connecting a high earth resistance is better for overvoltage protection when using a MOV surge arrester SPD to protect the load. The voltage fall time and clamping voltage of the MOV shows better performance when connected to a higher earth resistance. However, the MOV shows it reacts more quickly towards a surge when it is connected to a lower earth resistance due to the higher peak voltage being reflected across the MOV. These results both are considered valid as it holds true to the potential divider hypothesis that is mentioned in the report.

TABLE OF CONTENTS

DECLARATION	2
APPROVAL FOR SUBMISSION	3
ACKNOWLEDGEMENTS	5
ABSTRACT	6
TABLE OF CONTENTS	i
LIST OF TABLES	iii
LIST OF FIGURES	iv
LIST OF SYMBOLS / ABBREVIATIONS	vii
LIST OF APPENDICES	viii

CHAPTER

1	INTRODUCTION	1
	1.1 General Introduction	1
	1.2 Importance of the Study	1
	1.3 Problem Statement	2
	1.4 Aim and Objectives	2
	1.5 Scope and Limitation of the Study	2
2	LITERATURE REVIEW	3
	2.1 Introduction	3
	2.2 Surge	3
	2.2.1 External Source of Surge-Lightning	3
	2.2.2 Internal Source of Surge-Switching	7
	2.2.3 Characterization of Surge Waveform	9
	2.2.4 Effects due to Surge	11
	2.3 Surge Protection Device (SPD)	12
	2.3.1 Working Principle	13
	2.3.2 Protection Modes	14
	2.3.3 Classifications of SPD	14
	2.3.4 Crowbar and Clamping Device	16
	2.3.5 Gas Discharge Tube (GDT)	19
	2.3.6 Metal Oxide Varistor (MOV)	20
	2.4 Earthing	21

	2.4.1	Importance of Earthing	21
	2.4.2	Types of Earthing System	22
	2.4.3	Earth Electrode System	27
	2.4.4	Measurements of Earthing System	30
3		METHODOLOGY AND WORK PLAN	32
	3.1	Introduction	32
	3.2	Surge Generator Model	32
	3.3	Network Model	32
	3.4	Earthing Impedance	33
	3.5	SPD	33
	3.6	Parameters of Study	33
4		RESULTS & DISCUSSION	34
	4.1	Introduction	34
	4.2	Surge Waveforms	34
	4.3	MOV Simulation	39
	4.4	MOV Voltage Fall Time	42
	4.5	MOV Reaction Time	44
	4.6	MOV Clamping Voltage	46
	4.7	High Impedance Earth	48
5		CONCLUSION AND RECOMMENDATIONS	51
	5.1	Conclusion	51
	5.2	Recommendations	52
5		REFERENCES	53
5		APPENDICES	54

LIST OF TABLES

Table 2.1: Soil and electrode resistance according to soil type	30
Table 4.1: Comparison table for overvoltage surge	37
Table 4.2: Comparison table for overcurrent surge	38
Table 4.3: MOV peak voltage and fall time	43
Table 4.4: MOV voltage vs potential across earth resistance	44
Table 4.5: Reaction time of MOV for different earth resistances	46
Table 4.6: Steady state clamping voltage of MOV	47

LIST OF FIGURES

Figure 2.1: Charge separation of cloud and induced charge in the ground	4
Figure 2.2: Types of cloud discharge	4
Figure 2.3: Inductive coupling	6
Figure 2.4: Resistive coupling	7
Figure 2.5: Capacitive coupling	7
Figure 2.6: Relationship between current & magnetic flux for induced e.m.f	8
Figure 2.7: Capacitor switching transient	9
Figure 2.8: General impulse waveform	9
Figure 2.9: 1.2/50 μ s waveform	10
Figure 2.10: 8/20 μ s waveform	10
Figure 2.11: 100/350 μ s waveform	11
Figure 2.12: Burnt IC due to surge	12
Figure 2.13: Operation of SPD diverting surge to ground	13
Figure 2.14: Protection modes in wye and delta connection	14
Figure 2.15: Classifications of SPD	15
Figure 2.16: Type 1 SPD with impulse current rating of 25 kA	15
Figure 2.17: Type 2 SPD with impulse current rating of 20 kA	16
Figure 2.18: Type 3 SPD with impulse current rating of 5 kA	16
Figure 2.19: Gas Discharge Tube (GDT)	17
Figure 2.20: Voltage response according to different types of SPD operation	18
Figure 2.21: Metal Oxide Varistor (MOV)	18
Figure 2.22: Burnt MOV due to overheating	19

Figure 2.23:	Avalanche effect	19
Figure 2.24:	Resistance curve of MOV	20
Figure 2.25:	Clamping characteristic of MOV	21
Figure 2.26:	Fault current flow into the body due to disconnected earth wire	22
Figure 2.27:	Three-phase TT earthing arrangement	24
Figure 2.28:	Three-phase TN-C-S earthing	24
Figure 2.29:	Three-phase TN-C earthing	25
Figure 2.30:	Three-phase TN-S earthing	26
Figure 2.31:	Three-phase IT earthing	26
Figure 2.32;	Earth fault loop	27
Figure 2.33:	Model for soil resistance calculation	28
Figure 2.34:	Setup for 4-pin Wenner Test	31
Figure 3.1:	Surge generator model	32
Figure 3.2:	Network model	33
Figure 4.1:	Complete surge generator circuit model	34
Figure 4.2:	Front time of 1.2/50 μ s overvoltage surge waveform	37
Figure 4.3:	Tail time of 1.2/50 μ s overvoltage surge waveform	37
Figure 4.4:	Front time of 8/20 μ s overcurrent surge waveform	38
Figure 4.5:	Tail time of 8/20 μ s overcurrent surge waveform	38
Figure 4.6:	Surge applied onto the electrical network	39
Figure 4.7:	Voltage waveform across load	39
Figure 4.8:	MOV connected across load	40
Figure 4.9:	Surge waveform with MOV (yellow) & without MOV (blue)	40
Figure 4.10:	Clamped surge voltage	41

Figure 4.11:	Clamped surge voltage (zoomed in)	41
Figure 4.12:	Time taken for MOV voltage to drop to 400 V	42
Figure 4.13:	MOV voltage falling to 400 V for different earth resistance	43
Figure 4.14:	Time taken for MOV to react towards surge	45
Figure 4.15:	Reaction time of MOV for different earth resistances	45
Figure 4.16:	Steady state clamping voltage of MOV	47
Figure 4.17:	Steady state clamping voltage of MOV for different earth resistance	47
Figure 4.18:	High impedance earth network	48
Figure 4.19:	Voltage waveform of MOV with 20 Ω earth resistor (blue) vs 1 M Ω earth resistor (yellow)	49
Figure 4.20:	Voltage waveform of earth resistor (blue) vs voltage across MOV (yellow)	49
Figure 4.21:	MOV voltage waveform with 1000 Ω earth resistance	50

LIST OF SYMBOLS / ABBREVIATIONS

A	area
C	capacitance
GDT	gas discharge tube
MOV	metal oxide varistor
P	resistivity of soil
R	resistance
R_{earth}	earth resistance
R_{mov}	internal resistance of metal oxide varistor
SPD	surge protection device
t_{fall}	fall time of metal oxide varistor
V_{mov}	voltage across metal oxide varistor
V_{surge}	surge voltage

LIST OF APPENDICES

Appendix A: IEEE C62.41.2 STANDARD	54
------------------------------------	----

CHAPTER 1

INTRODUCTION

1.1 General Introduction

A surge, in general, can be understood as a sudden gush of energy that disrupts everything on sight. In an electrical sense, a surge is a sudden rush of energy being introduced into the system either externally or internally. An electrical surge causes damage to systems and hence a device that protects against surge such as a surge protection device (hereinafter SPD) is essential. The main function of an SPD is to divert the surge into the earth instead of flowing into the system. With that being said, deviations of the earth would affect the operation of the SPD to some degree. In this project, studies on how earthing deviations would affect the performance of the SPD is conducted.

1.2 Importance of the Study

The event of a surge cannot be predicted, and this is dangerous as it is not within our scope of control. Surges can cause damage to sensitive electronic systems or even halt essential services that require a 24/7 power supply. In this day and age where electrical systems are implemented in industries such as the communication sector or web data storage centres, they are at risk of damage and downtime due to the occurrence of surge. Downtime in such industries can be a financial burden for businesses; hence surge protection technologies are developed to protect such systems from failing due to surges.

The implementation of SPD can provide quick and responsive protection towards surges in both electrical and electronic systems. However, due to the nature of operation of the SPD, the performance of the device to some extent is affected by the earthing system of which it is installed on. As the SPD diverts the surge into the earth, the SPD coordinates with the earthing system to provide efficient and responsive surge protection. Therefore, it is important to understand how earthing deviations would affect the performance of the SPD.

1.3 Problem Statement

As mentioned before in the previous subchapter, the SPD and the earthing system are two elements that operate harmoniously with one another. This project is done to study the factors of the earthing system that may compromise the overall performance of an SPD.

1.4 Aim and Objectives

The main objective of this project is to study the effects of earthing deviations that would affect the performance of the SPD. The breakdown of the objectives is:

- i. Perform studies on electrical surges.
- ii. To investigate the voltage characteristic of the SPD when diverting surges on different earth impedance.
- iii. To investigate the time taken for the SPD to react to surges on different earth impedance.

1.5 Scope and Limitation of the Study

For the scope of the study, the surge waveform that will be simulated and carried out on the hardware prototype would be that of a surge due to an indirect lightning strike which follows the 1.2/50 μ s and 8/20 μ s waveform as defined by IEC 61000-4-5. A surge waveform of a direct lightning strike (100/350 μ s waveform) is not simulated nor it is tested on the hardware prototype in this study as a direct lightning strike is beyond our scope of control.

The complete and detailed studies on the topic of earthing is very complex and existing research on earthing analysis is still quite vague as at the time of writing this report. Hence, the project will be based on existing published papers done by previous researchers.

CHAPTER 2

LITERATURE REVIEW

2.1 Introduction

The many sources and characteristics of surges will be studied in this chapter. Different types of modern-day surge protection schemes on surges will also be explored. Detailed studies on electrical grounding as well as the elements of grounding that would affect the SPD will also be reviewed.

2.2 Surge

Surge is described as a sudden spike of voltage or current in a system. The source of surge can originate from either within or outside the system. There is a multitude of effects of surge that includes damaging assets or even threaten human safety.

2.2.1 External Source of Surge-Lightning

Phenomenas that induces a surge which originates outside the electrical system is considered as an external source of surge. The most common external source of surge is the occurrence of lightning. A lightning event can induce surges either directly or indirectly onto electrical systems.

2.2.1.1 Surges due to Direct Lightning Strike

Lightning is the most common source of surge that is experienced every day in the entire world. To put it to perspective, the number of lightning strikes that hit the surface of the earth is approximately 9,000,000 lightning strikes in a day. The mechanism of which how lightning is formed can be explained by first understanding what lightning is. Lightning can be defined as a long electrical spark that stretches across the sky between clouds in the atmosphere. The long electric spark can also occur between a cloud and the earth's surface. These electrical sparks exist due to the interaction of minor ice and water molecules that are condensed inside a cloud. The ice and water molecules collide with one another and eventually polarized themselves making the ice particles positively charged whilst the water molecules become negatively charged. Due to the

nature of the water molecules in the cloud being heavier than the ice particles, the polarized water molecules tend to shift to the bottom half of the cloud while the lighter polarized ice particle shifts to the top half of the cloud. This would eventually contribute to a separation of charge in the cloud whereby the cloud is negatively charged on the bottom, whilst the top is positively charged as depicted in Figure 2.1. There are a few ways for the cloud to discharge all its accumulated charges; Mainly through the cloud to ground discharge (cloud to ground lightning), discharge within the cloud itself (intracloud lightning), between two charged clouds (intercloud lightning), and many more as depicted in Figure 2.2. (Uman, Martin.A., 2008)

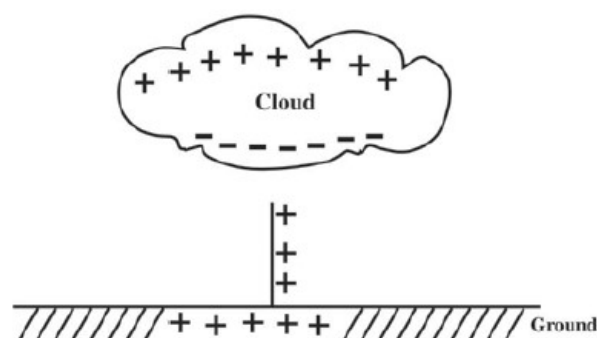


Figure 2.1: Charge separation of cloud and induced charge in the ground (Vijayaraghavan, G., Brown, M., Barnes, M., 2004)

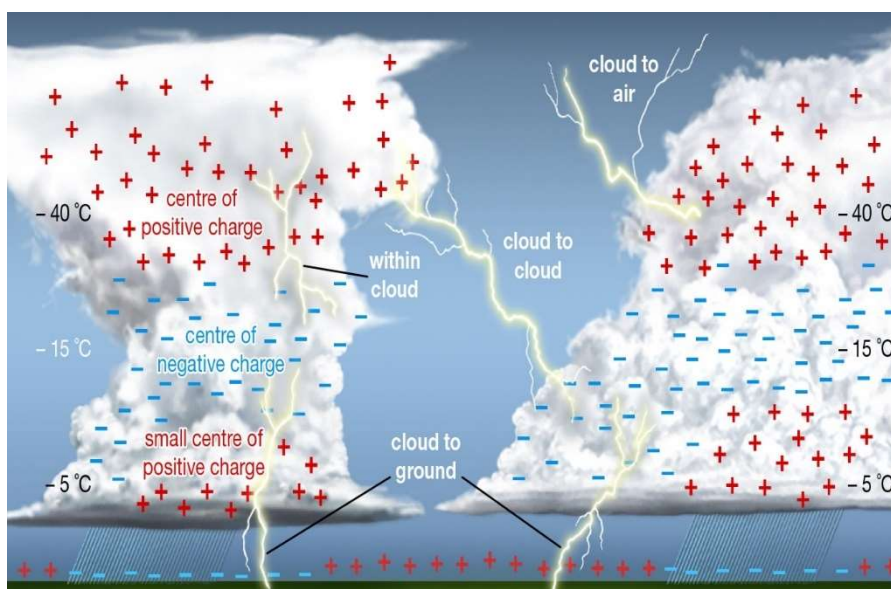


Figure 2.2: Types of cloud discharge (Encyclopedia Britannica, 2020)

With regards to cloud to ground discharge, following the charge separation of a cloud, the negatively charged bottom portion of the cloud would induce the nearby earth surface beneath to be positively charged as depicted in Figure 2.1. Due to the induced ground charges being of opposite polarity to the bottom portion of the cloud, there exists a high level of electric field in the space between the cloud and the ground. The air molecules that are present in said space experience high levels of electric field and eventually breaks down. The process of air molecules breaking down due to the immense level of electric field is called Ionization. The air molecules are said to be ionized and lose all its insulating properties which subsequently acts as a short circuit and creates a conducting path connecting the cloud to the ground. Subsequently, this would lead to the discharge of charges from the cloud to the ground through the ionized path. Thus, it can be said that a lightning strike from the cloud to the ground has occurred. (Vijayaraghavan, G., Brown, M., Barnes, M., 2004)

2.2.1.2 Surges due to Indirect Lightning Strike

When a cloud to ground discharge occurs, it indirectly causes an effect of inducing surges in the vicinity of the area where the lightning struck. The surge level due to an indirect lightning strike is significantly lesser than its counterpart but its frequency of occurrence is higher as the surge can propagate to a wider area than that of a direct lightning strike.

Induced surges due to indirect lightning strikes are mainly caused by coupling effects on the objects which are in the vicinity of the discharging cloud. The coupling effect can be categorized into three main subjects: inductive coupling, resistive coupling, and capacitive coupling.

In general, high rise buildings would have a lightning rod installed on the top of the roof of the building for lightning protection. The lightning rod acts as a down conductor to divert the surge caused by the lightning strikes into the ground, preventing any harm on humans or appliances within said building. When the lightning strikes the down conductor, a magnetic field would be induced due to the sudden change in potential across the down conductor. Inductive coupling occurs when the cables nearby the down conductor picks up the magnetic field and indirectly induces a surge of voltage. The cables which would induce a surge when the down conductor is struck by lightning are said

to be inductively coupled together with the down conductor. Inductive coupling is depicted as shown in Figure 2.3.

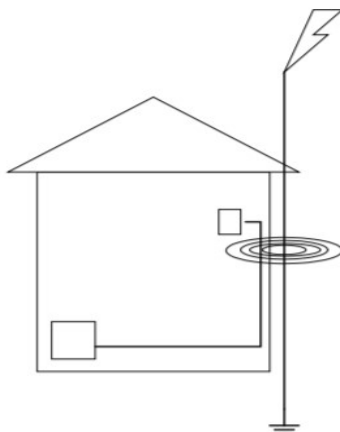


Figure 2.3: Inductive coupling

Following the scenario above, when the lightning rod diverts the high lightning current into the ground, the ground potential which ideally should be zero would rise. As depicted in Figure 2.4, high lightning currents flow into the ground through the lightning rod and this would lead to a rise in ground potential in that particular area. When the ground potential near the lightning rod is raised, there exists a potential difference across the entire vicinity of the area whereby the ground potential nearer to the lightning rod would be higher; whilst areas which are located further away would have a relatively low ground potential. The difference in ground potential would indirectly induce a surge that would propagate through the earthing system or the underground cables and eventually, would disturb the entire electrical system. As a result, the nature of which how a difference in ground potential would indirectly induce a surge into an electrical system is described as resistive coupling. (Kawamura, Takeshi Harada, Isao Matsushita, Tomohisa, 1991)

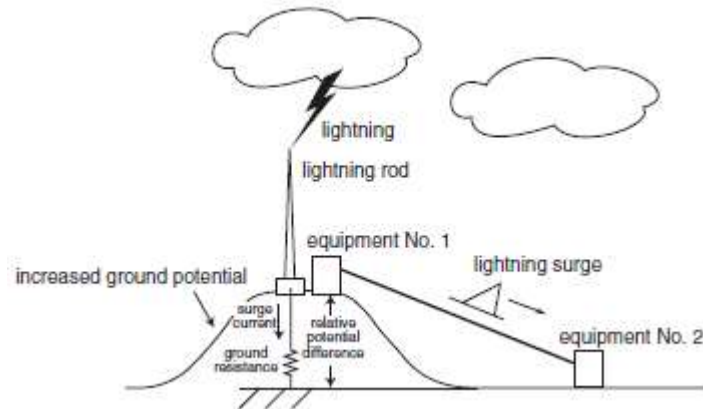


Figure 2.4: Resistive coupling

Another structure that is prone to lightning strikes is overhead transmission lines that span kilometers in length. When lightning strikes a transmission line, the surge is propagated throughout the entire transmission system which subsequently causes any adjacent victim transmission wires to be capacitive coupled as depicted in Figure 2.5 below.

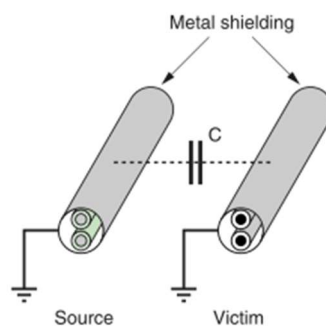


Figure 2.5: Capacitive coupling

2.2.2 Internal Source of Surge-Switching

Phenomenas that induces a surge which originates from the inside of the electrical system is considered as an internal source of surge. The most common internal source of surge is due to switching of loads, either capacitive loads or inductive loads. Surges caused by switching of loads can be commonly observed in our daily lives. One such instance is when switching on an air-conditioning unit, the lights which are connected to the same electrical system tend to flicker as the electrical demand is fluctuating. Besides switching of large electrical appliances, small electronic devices that integrate the use of high-frequency

switching devices such as transistors often cause frequent low-level surges that contribute to noise.

2.2.2.1 Inductive Load Switching

Most loads that can be found commercially used in the market are generally inductive. During switching operation, the sudden fall of magnetizing current causes the rate of change of magnetic flux to increase and thus contributes to the rise of induced e.m.f in the coil as depicted in Figure 2.6 below. The induced e.m.f is disproportionately high during switching operations and results in unwanted internal surge. (Agrawal, K.C., 2001)

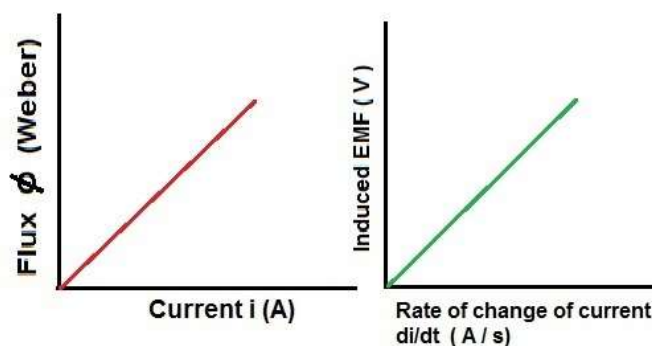


Figure 2.6: Relationship between current and magnetic flux or induced e.m.f
(topperlearning, 2017)

2.2.2.2 Capacitive Load Switching

To compensate for the lagging power factor caused by inductive loads, capacitor banks are often installed onto the power system grid to improve the overall power factor of the system. By installing capacitor banks which has a leading power factor, power factor corrections can be done by compensating the lagging power factor of the system to raise the overall efficiency of delivering power. Capacitor banks are often switched on and off depending on the need to perform power factor correction. The main downside of implementing capacitor banks is the nature of capacitor switching which will produce oscillatory transients that would contribute to internal surges in the system. Figure 2.7 below depicts an overvoltage transient when the instant capacitor switching occurs. (Low, K.S, 2018)

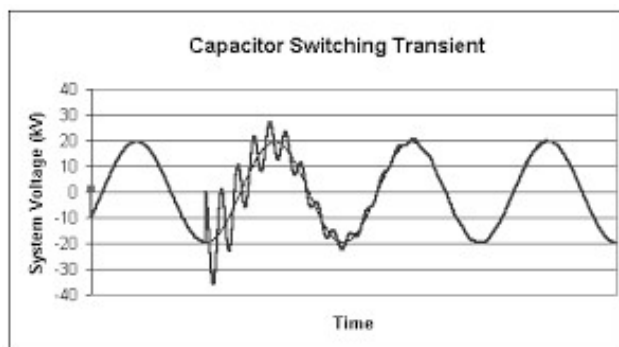


Figure 2.7: Capacitor switching transient (Nepsi, 2012)

2.2.3 Characterization of Surge Waveform

To describe a surge, the general impulse waveform as shown in Figure 2.8 is used. A standard impulse waveform is generally unidirectional and is skewed to the right. The maximum value of the waveshape is the peak impulse voltage or current of the surge. The impulse voltage waveform can be described using an equation which combines two exponential waveforms such as

$$V = V_0(e^{-\alpha t} - e^{-\beta t})$$

Where α and β represent constants in microsecond units. The equation above gives a waveform that rapidly rises to its peak and gradually falls to zero over time, similar to how a surge waveform should look like.

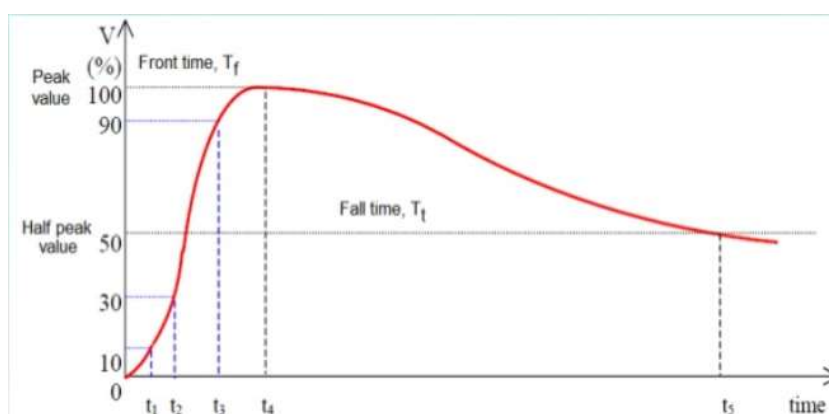


Figure 2.8: General impulse waveform (Fotis, G. P., Gonos, I. F., Stathopoulos, I. A., 2004)

An impulse waveform is characterized by its peak value and its two time intervals: the front time and the tail time. The front time t_f represents the time taken for the waveform to achieve its peak value; whereas the tail time t_t

represents the time taken for the waveform to decay to half of its peak value. According to IEC 61000-4-5, lightning impulse waveforms can be categorized into three waveforms with different t_f and t_t combinations: 1.2/50 μs , 8/20 μs , and 100/350 μs waveforms.

A 1.2/50 μs impulse waveform as depicted in Figure 2.9 is used to describe voltage surges caused by indirect lightning strikes. The period of which the surge lasts is also shorter to a direct lightning strike. According to IEC 61000-4-5, a voltage surge waveform caused by an indirect lightning strike achieves its peak voltage at 1.2 μs and decays to half of its peak value in 50 μs .

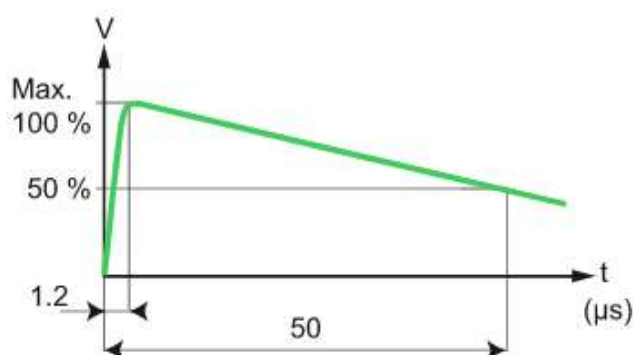


Figure 2.9: 1.2/50 μs waveform (electricalinstallationwiki, 2019)

An 8/20 μs impulse waveform as show below in Figure 2.10 is used to describe the current surges that are accompanied with the voltage surges caused by indirect lightning strikes. According to IEC 61000-4-5, a current surge waveform caused by an indirect lightning strike has a front time of 8 μs and a tail time of 20 μs .

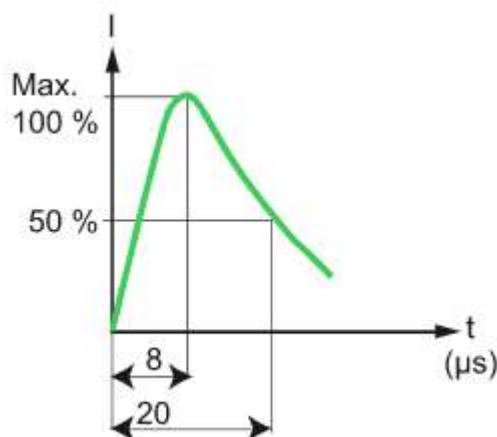


Figure 2.10: 8/20 μs waveform (electricalinstallationwiki, 2019)

A 100/350 μs impulse waveform shown in Figure 2.11 is used to describe voltage surges caused by direct lightning strikes. The period of which the surge lasts is also longer compared to an indirect lightning strike. According to IEC 61000-4-5, a voltage surge waveform caused by a direct lightning strike achieves its peak voltage at 100 μs and decays to half of its peak value in 350 μs . Compared to an indirect lightning strike, a direct lightning strike is more severe and the devastating effects that comes with it last longer.

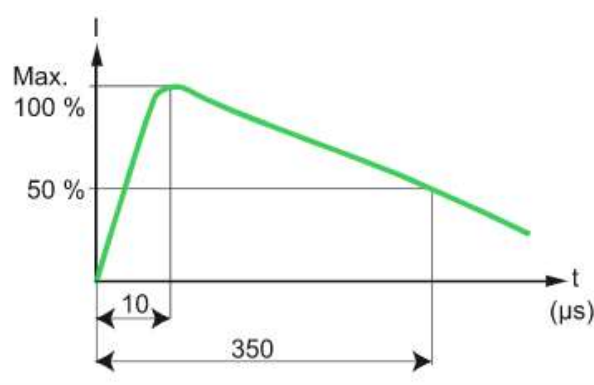


Figure 2.11: 100/350 μs waveform (electricalinstallationwiki, 2019)

2.2.4 Effects due to Surge

The occurrence of surge due to switching devices often creates unintended switching surges or noise within the electrical system. In communication systems, the presence of noise interferes with the proper flow of signal being transmitted or received and this affects the efficiency of decoding the signals and messages.

Noise also interferes with the quality of power being delivered into equipment that uses a motor. When the current flowing into a motor is constantly being fluctuated by electrical noises due to switching surge, the motor would not be able to run optimally at a constant speed and experience both electrical and mechanical stress. This would eventually lead to the degradation of the machine.

Besides that, due to the sudden increase in both voltage and current, electronic equipment that has a low power rating would get overheated. Overvoltage caused by surge happens almost instantaneously and the voltage regulators embedded in the device may not be able to handle the sudden

transient overvoltage and eventually, the important electronic equipment may burn as shown below in Figure 2.12.

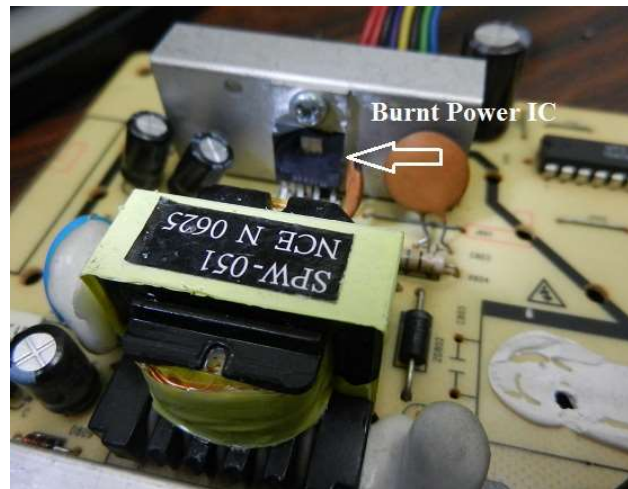


Figure 2.12: Burnt IC due to surge

In heavy industrial sectors, a surge can cause devastating effects to the personnel that is working in the process plant. Industrial sectors such as oil and gas extraction plants that rely heavily on electrical power cannot afford to sustain a surge as many essential pieces of machinery that are sensitive to overvoltage and overcurrent in the plant would stop operating. This would lead to unwanted downtime or even compromise the safety of employees that are working in extreme conditions. For example, in the United States, it is noted by the National Lightning Safety Institute (NLSI) that a lightning surge incident caused a warehouse in Denver to lose approximately \$50 million in total assets.

There are still plenty of consequences of surge that are not discussed in this section. However, it provides a reasonable perspective on what are the effects of surge in our daily lives.

2.3 Surge Protection Device (SPD)

A surge protection device is a device that is installed to prevent surge current or voltage from entering a piece of equipment or electrical system and inflicting damages. SPD which are commonly used include the Metal Oxide Varistor (MOV) and the Gas Discharge Tube (GDT).

2.3.1 Working Principle

In practice, SPD are installed at the input of the equipment, parallel to the load that is to be protected by surge as depicted in Figure 2.13. The impedance of an SPD is inversely proportional to the voltage across it. This means that in an event where the voltage across the SPD is above a certain threshold, the impedance of the SPD decreases drastically to a point where it acts like a shorted wire connecting the phase conductor to the earth. When this happens, instead of the surge current flowing into the device, it takes the path of least resistance and flows down to the earth through the SPD. The SPD is said to divert the surge to the ground and thus protects the device. When the voltage across the SPD is back to its initial normal value, the SPD would restore its high impedance property to prevent leakage current to earth. Hence, the general principle of proper operating SPD are:

1. Provide low impedance path during surge events to divert surge to earth.
2. Remain high impedance property to minimize leakage current to earth during normal operation.
3. Respond faster than typical circuit breakers to divert surge in time.
4. Restore high impedance property after diverting surge to earth.

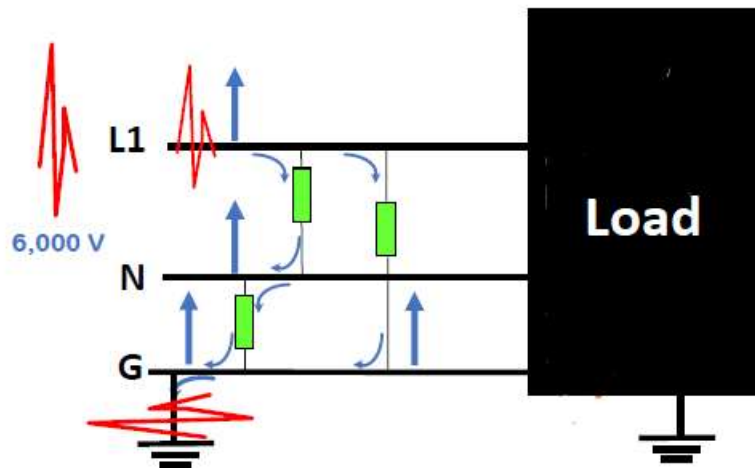


Figure 2.13: Operation of SPD diverting surge to ground

2.3.2 Protection Modes

During a surge, the overcurrent may flow in two modes: Differential mode and Common mode. Referring to Figure 2.14 below, in differential mode, the surge current flows from one phase conductor to another, whereas in common mode, the surge current flows from phase conductor to earth.

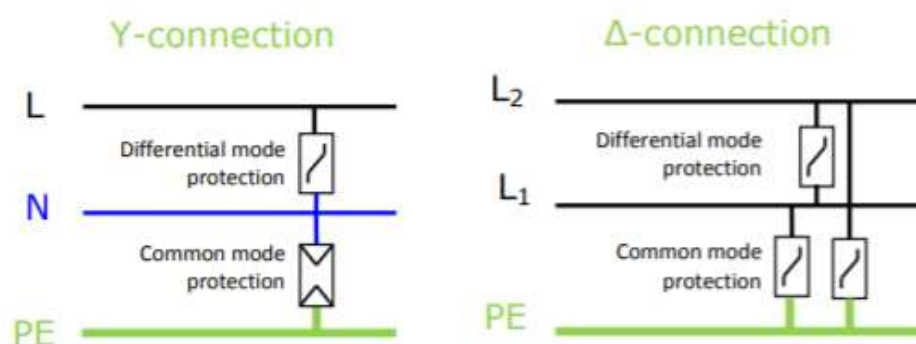


Figure 2.14: Protection modes in wye and delta connection (Eltek, n.d.)

In differential mode protection, the SPD matches the amount of current between two conductors. In the case where there is a surge, one of the phase conductors would experience a higher amount of surge current and the SPD will notice the difference between the two conductors and diverts the surge current from reaching the equipment.

In common mode protection, the SPD is connected in between the phase conductor and earth. In case of surge, the SPD activates and diverts the surge current from the phase conductor to the ground, preventing the equipment from harm.

2.3.3 Classifications of SPD

According to IEC 61643-1 Performance Requirements of Surge Protective Devices for Low-Voltage Power Supply Systems, SPD are generally categorized into three main types: Type 1, Type 2, and Type 3 as shown in Figure 2.15.

type of SPD	IEC 61643-11 (2011-03)
SPD for lightning equipotential bonding	SPD test class I
SPDs for protection against transient overvoltages	SPD test class II
SPDs for protection against transient overvoltages and for equipment protection	SPD test class III
SPDs with filter for enhanced equipment protection	IEC 61000-4-5

Figure 2.15: Classifications of SPD (Zotup, n.d.)

Type 1 SPD depicted below in Figure 2.16 is characterized by a 10/350 μ s impulse current waveform. Type 1 SPD have a higher surge current rating and is used for protection against direct lightning strikes. Examples of Type 1 SPD are lightning current arresters.



Figure 2.16: Type 1 SPD with impulse current rating of 25 kA (Confly, n.d.)

Type 2 SPD as shown in Figure 2.17 is characterized by an 8/20 μ s impulse current waveform. Type 2 SPD are used as the main protection against indirect lightning effects on low voltage electrical installations.



Figure 2.17: Type 2 SPD with impulse current rating of 20 kA (Confly, n.d.)

Type 3 SPD is characterized by a combination of 1.2/50 μ s impulse voltage waveform and an 8/20 μ s impulse current waveform. Type 3 SPD depicted in Figure 2.18 have lower surge current rating and hence are generally supplemented by a Type 2 SPD. Type 3 SPD are generally used as protection against switching overvoltage.



Figure 2.18: Type 3 SPD with impulse current rating of 5 kA (Confly, n.d.)

2.3.4 Crowbar and Clamping Device

Generally, an SPD can operate as either a crowbar device or a clamping device. As a crowbar device, it gets its name from the idea of dropping a metal crowbar across two phase terminals, short-circuiting the system. An SPD which

operates as a crowbar device normally has highly conductive gasses in them. These gas particles, when exerted on high voltage, will ionize and breakdown in a sequence of avalanche effect. This avalanche effect eventually causes the insulating properties of the SPD to fall drastically and provide a short-circuited path for the fault current to flow into the ground.

The drawback of an SPD operating as a crowbar device is the power supplied to the load will be cut off. As the SPD short circuits the incoming power during the surge, there is no current flowing into the load and thus no power is being delivered to the load. Crowbar devices are not recommended to be installed at the input terminals of essential loads such as hospitals or hazardous industry sectors as a power outage can cause immense consequences. Besides that, crowbar devices generally have a slower response time when it comes to diverting surge to the ground as the avalanche process of breaking down the insulation level of the SPD requires time. Examples of commonly used SPD which are operating as crowbar devices are Gas Discharge Tubes (GDT) as depicted below in Figure 2.19 and Silicon Control Rectifier (SCR).



Figure 2.19: Gas Discharge Tube (GDT) (Epcos, n.d.)

On the other hand, SPD operating as clamping devices does not short the phase conductor to the ground completely during a surge. Instead, the SPD clamps the voltage level across it to a certain predefined level to limit the amount of current flowing into the load. A clamping device operates in such a way to split the incoming current; diverting the surge current to ground while still allowing some amount of current to flow into the load.

For a clamping type SPD, when surge voltage is experienced across the terminals of the SPD, the impedance of the SPD falls rapidly to a certain extent, allowing the excess surge current to flow to the ground while still maintaining

the voltage across its terminals and not completely short circuiting it as shown in Figure 2.20.

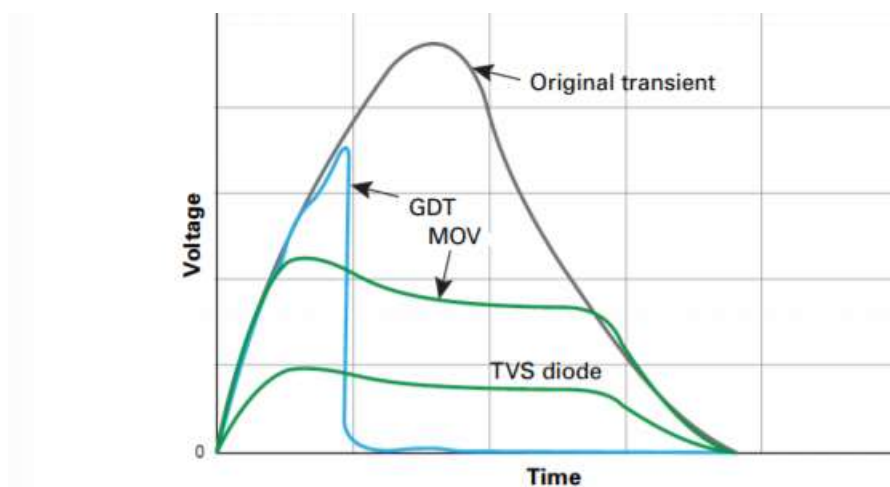


Figure 2.20: Voltage response according to different types of SPD operation

The disadvantage of a clamping type SPD is the amount of heat generated during discharge. As a clamping device SPD only restricts the amount of current flowing into the load by lowering its impedance and diverting the excess surge current to ground, the high level of surge current that flows through the SPD is dissipated as heat as there is still a certain level of internal resistance in the SPD. The effects of overheating due to prolonged exposure to surge current on an SPD as a clamping device is shown in Figure 2.22. However, the response time of a clamping type SPD is faster than that of a crowbar SPD. Examples of commonly used SPD which are operating as clamping devices are Metal Oxide Varistor (MOV) depicted in Figure 2.21 and Zener diodes.



Figure 2.21: Metal Oxide Varistor (MOV)



Figure 2.22: Burnt MOV due to overheating (electronicsrepair, n.d.)

2.3.5 Gas Discharge Tube (GDT)

A Gas Discharge Tube (hereinafter GDT) is a crowbar type SPD. The internal mechanism of GDT consists of two electrodes separated by a highly ionizable gas within a chamber. The gas that fills the chamber is generally of Group 18 noble gas mixture. When the terminals of the GDT experienced an overvoltage due to surge, gasses within the chamber are ionized and liberates free electrons. The free-electron will accelerate towards the other terminal and in the process, collides with another gas-particle and ionizes them. This ionization process is repeated many times and is known as the avalanche effect as depicted in Figure 2.23. Once the gas particles in the GDT are ionized, it provides a conducting path and arcing across the two electrodes occurs. Hence, during overvoltage, the gas inside GDT breaks down becomes very conductive, acting like a short circuit diverting the overcurrent to the ground.

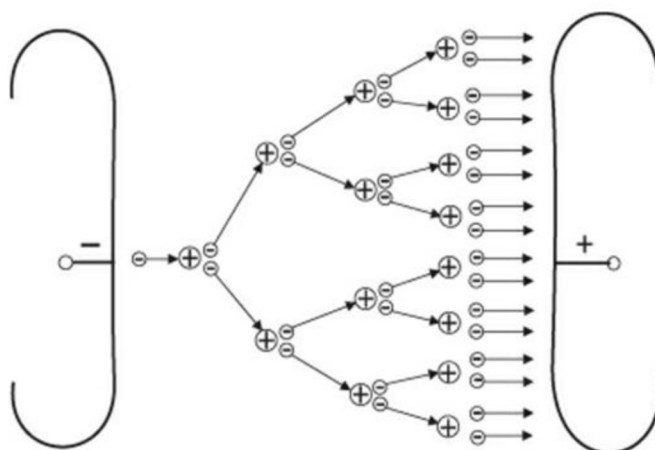


Figure 2.23: Avalanche effect

During normal conditions, the voltage across the terminals of the GDT is not high enough to ionize the gasses in the chamber. Therefore, the insulation of the gasses remains and GDT does not conduct during normal voltage levels.

2.3.6 Metal Oxide Varistor (MOV)

A Metal Oxide Varistor (hereinafter MOV) is a clamping type SPD which consists of metal oxide components in between two electrodes. The characteristic of the MOV is very dependent on the voltage across its terminals. The resistance curve of the MOV against the voltage is depicted in Figure 2.24.

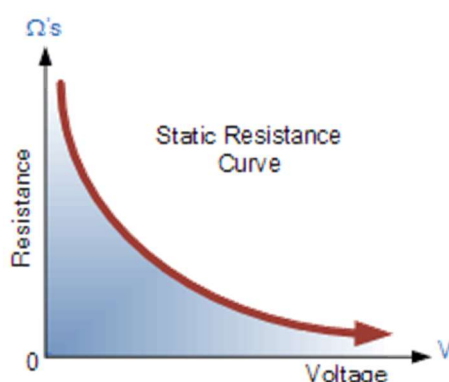


Figure 2.24: Resistance curve of MOV (electronicstutorials, n.d.)

The resistance of the MOV is ideally infinite during normal voltage levels. It can be seen from the resistance curve above that as the voltage across the MOV terminal increases, the resistance falls drastically. This characteristic of the MOV makes it suitable to protect a device from surge as, during normal voltage level, the high impedance of the MOV makes it such that the MOV does not exist in the system. However, in an overvoltage event, the surge of voltage will induce the resistance of the MOV to fall drastically to divert a certain amount of surge current from entering into the system and cause damage.

Unlike the GDT, the MOV does not completely short circuit the phase conductor to the ground. Instead, it reduces its resistance value to clamp the voltage to a specific designated value as shown in Figure 2.25.

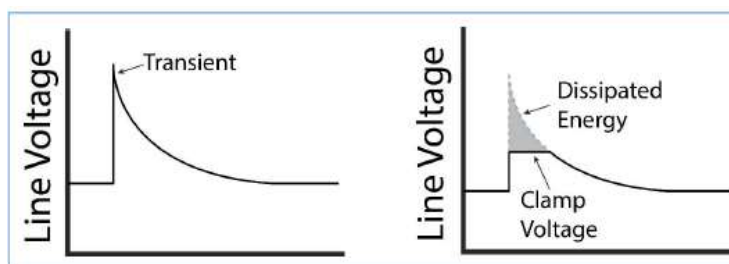


Figure 2.25: Clamping characteristic of MOV

As there still exists some internal resistance due to the metal oxide compounds in the MOV, when diverting surge current, the energy is mostly dissipated as heat. This indicates that the MOV tends to overheat over time.

2.4 Earthing

The idea of earthing has always been around since the early days of implementing electrical systems. The terminology “earthing” and “grounding” are often confused to describe a reference point of an electrical system. According to IEEE, the term “earthing” is used when there exists a circuit physically connected to the soil mass (earth) and takes the potential of the earth as a reference point. “Grounding” is generally used when the reference is with respect to other electrical points and may not be connected to the physical earth. To put it into perspective, in a high-rise building, the reference point for electrical connection on the tenth floor is the ground as it is not physically connected to the soil mass. Whereas the entire building itself uses the earth as a reference as it is solidly built on the soil mass. (Vijayaraghavan, G., Brown, M., Barnes, M., 2004)

2.4.1 Importance of Earthing

The implementation of earthing system is to provide 2 main purposes:

1. Provide electrical reference
2. Provide electrical protection

The electrical earthing system enables the measurement of voltage on a electrical with respect to the electrical reference. By connecting on the same level of electrical reference, the entire electrical system can be maintained on a standardized reference level. Without earthing, the voltages across multiple

points may be defined inconsistently as there is no standard reference point to refer to.

Earthing also protects against electrical faults that are prone to happen when dealing with electrical systems. Electrical appliances with metal enclosures are not normally energized. However, in case of fault whereby the insulator of the phase wire is exposed and is in contact with the metal enclosure, a person who comes in contact with the metal enclosure would get electrocuted due to the current flowing from the faulty equipment through the body as shown in Figure 2.26. The earth wire inside equipment with metal enclosures provide an alternate low impedance path for the fault current to flow into the earth directly, instead of passing through the human's body. The same concept applies to provide an alternate path for fault current to flow instead of flowing to the load during a lightning event which causes surges.

In short, earthing provides a standard electrical reference for the electrical system and allows fault currents to flow by providing an alternate low impedance path.

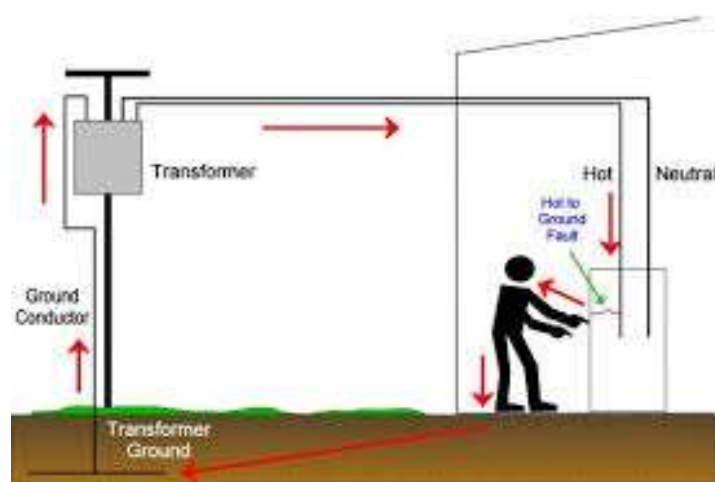


Figure 2.26: Fault current flowing into the body due to disconnected earth wire
(dengarden, 2020)

2.4.2 Types of Earthing System

Following BS 7671/ MS IEC 60364 Part 4, the five main types of earthing systems are

1. TT
2. TN-C-S

3. TN-C
4. TN-S
5. IT

The first letter indicates the type of connection that is made to earth on the source side.

- T: Derived from ancient Greek “Terra”, T stands for Terre or earth. This indicates that the system is directly connected to the source side earth.
- I: Represents Isolated. This indicates that the system has no connection to the earth or only connected through a high impedance.

The second letter indicates the type of connection that is made to earth on the load side.

- T: The system has a physical connection to load side earth.
- N: The system implements a neutral cable that connects both the source and load.
- C: The load system has a neutral cable which is combined with the earth cable.
- S: The load system has a neutral cable but is separated from the earth cable.

Under Malaysian Standard 1936:2016, TT and TN-S systems are typically used. TN-C-S and IT earthing arrangements are not permitted for low voltage systems while TN-C system is not permitted in Malaysia.

2.4.2.1 TT System

In TT system, the neutral of the source is connected physically to earth. However, the utility does not share this earth with the consumer. On the load side, the consumer provides their own connection to earth such as installing earth electrodes locally in their vicinity. The main advantage of a TT earthing system is there is minimal interference between the source and consumer as they are not sharing the same earth as reference. The TT system as shown in Figure 2.27 is the preferred method of earthing used applied in Malaysia and especially in communication industries where minimization of external interferences that corrupts the signal is of priority.

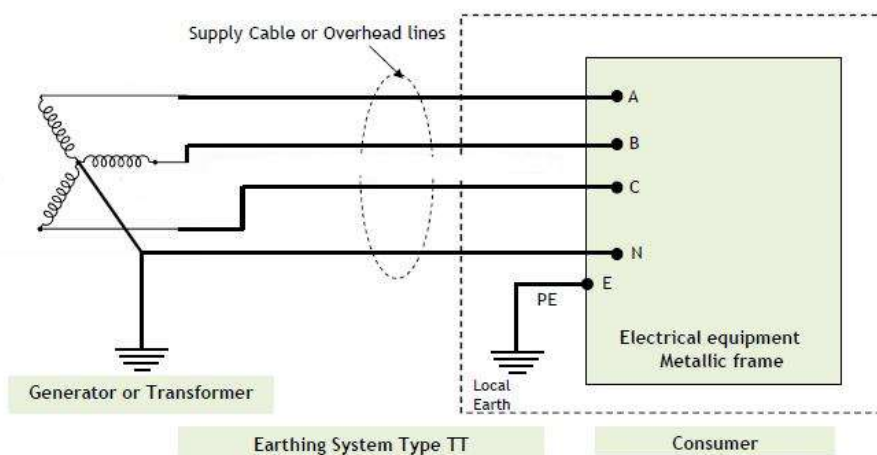


Figure 2.27: Three-phase TT earthing arrangement
(electricalengineeringtoolbox, 2015)

2.4.2.2 TN-C-S System

In TN system arrangements, the source neutral is connected physically to the soil mass at source side. Whereas at the load side, it is earthed through a protective earth conductor, better known as PE, which connects back to the source “earth”.

With this in mind, TN-C-S arrangement as depicted in Figure 2.28 has the supply neutral conductor combined with the PE as a single cable and is generally named the PEN (PE+N) conductor. While at the load side, the neutral and PE conductors are separated.

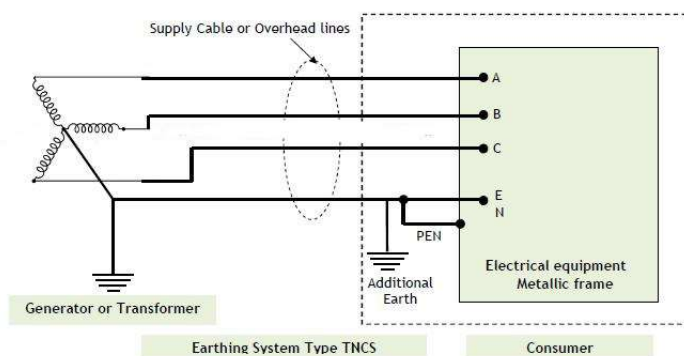


Figure 2.28: Three-phase TN-C-S earthing (electricalengineeringtoolbox, 2015)

2.4.2.3 TN-C System

In TN-C system as shown in Figure 2.29, the source is connected to the earth through a low impedance earth electrode. A single combined PEN conductor is used to connect the load side earth to the source. The disadvantage of this arrangement is due to the combined PE and N cable, the possibility of damaging the PEN would compromise the entire earthing system.

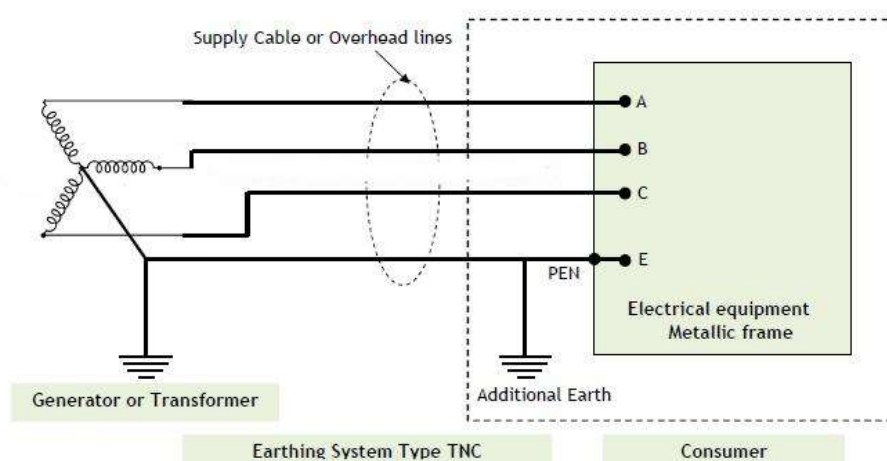


Figure 2.29: Three-phase TN-C earthing (electricalengineeringtoolbox, 2015)

2.4.2.4 TN-S System

In TN-S system, the source is connected to the earth through a low impedance earth electrode. Unlike the TN-C system, the PE and N conductors are separated both at the source side and load side as depicted in Figure 2.30. TN-S systems are considered among the safest earthing arrangement to implement as two separate conductors are providing an alternate path for fault current to flow. The main downside of the system is the implementation cost for two independent conductors stretching from the source side to the load side may be relatively higher.

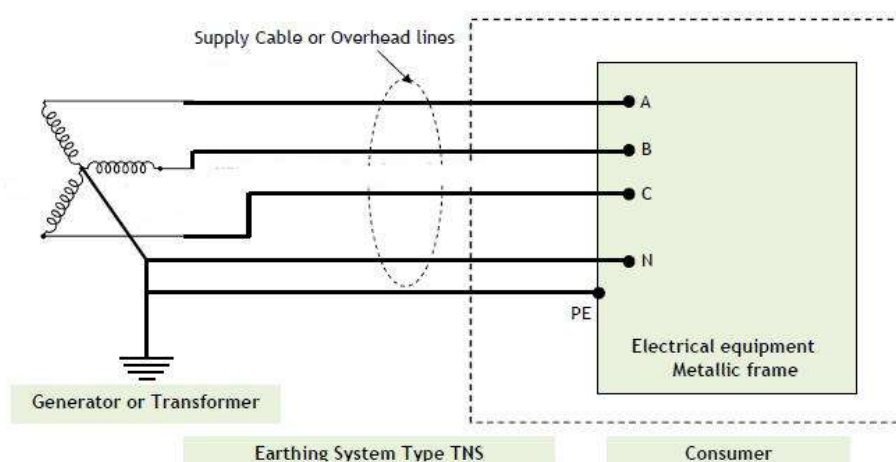


Figure 2.30: Three-phase TN-S earthing (electricalengineeringtoolbox, 2015)

2.4.2.5 IT System

The IT system as shown in Figure 2.31 implements two separate earth electrodes. However, unlike the TT system, the source neutral is said to be isolated as it is connected to the ground through high impedance.

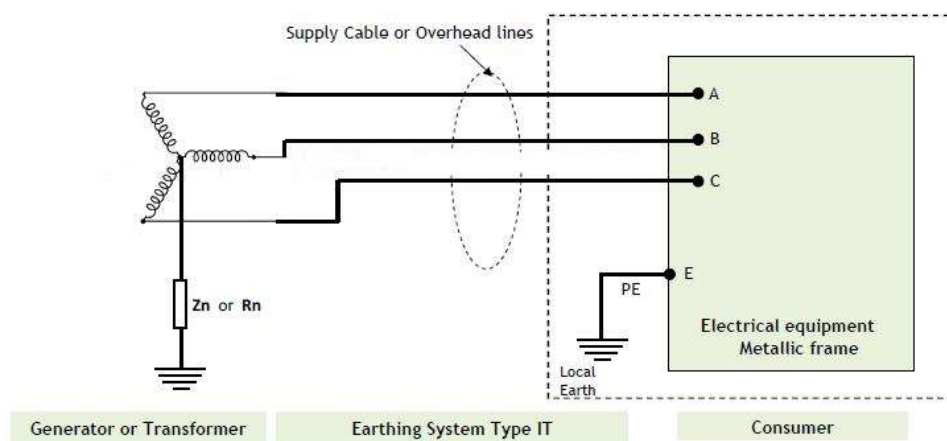


Figure 2.31: Three-phase IT earthing (electricalengineeringtoolbox, 2015)

The main characteristic of an IT earthing system is that at the load side, during a fault, the fault current will not operate the circuit breakers in the system as the fault current does not flow back to the source. Instead, in general, IT earthing installations, the main alarm lights up and identifies the location of fault for later inspection. This characteristic from an IT arrangement ensures continuous power supply to the load and hence can be found usually

implemented in industries where continuous power supply is of utmost importance such as hospitals. The major downside of IT arrangement is the implementation costs as detailed and precise planning shall be conducted for the Building Management System (BMS) to detect faults that may occur.

2.4.3 Earth Electrode System

In this section, the elements that are involved in an earthing electrode system, mainly what contributes to the overall ground resistance of the earthing system is discussed.

2.4.3.1 Earth Fault Loop Impedance

Taking a TT arrangement earthing system as an example, in the event of a surge of overcurrent or fault, the fault current would flow from the point of fault, down to the earth through the earth electrode installed, and completes the earth fault loop as depicted in Figure 2.32.

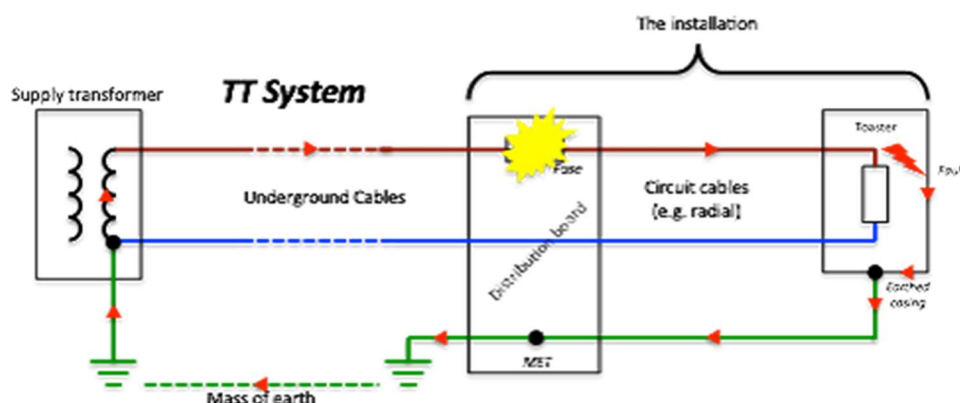


Figure 2.32; Earth fault loop (electronicteachingresources, n.d.)

The fault current flows through the earth mass back to the source due to its low impedance and thus the earth fault loop impedance must be low enough for the fault current to flow. High earth fault loop impedance is not desirable as it would contribute to lower fault currents and this would lead to the protection scheme not being able to pick up the fault and operate accordingly.

In the next following sub-chapters, the factors that will affect the overall earth fault loop impedance due to the earthing system will be discussed in detail.

2.4.3.2 Soil Resistance

The earth is assumed to be a sink that can absorb a large amount of current into it, which is why fault currents are usually directed into the earth. The earth itself consists of soil mass which has a definite amount of resistance. The model for soil resistance is shown in Figure 2.33. However, soil resistance is relatively low and it varies upon factors such as the following:

1. Presence of conductive minerals
2. Moisture of soil
3. Compactness of soil

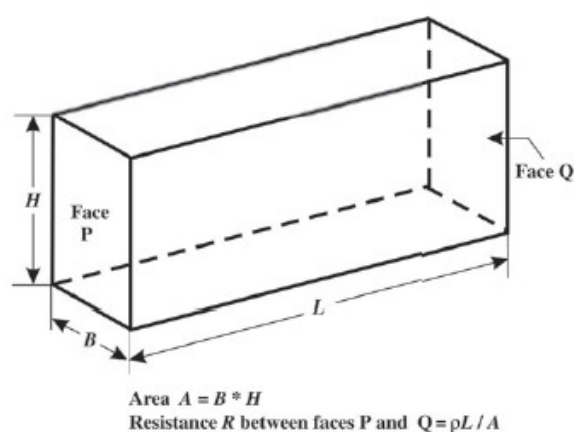


Figure 2.33: Model for soil resistance calculation (Vijayaraghavan, G., Brown, M., Barnes, M., 2004)

The soil resistance can be calculated using the formula:

$$R = \frac{\rho L}{A}$$

Where

- R: Resistance of soil across face P and Q
 ρ : Resistivity of soil
 L: Distance between face P and Q
 A: Surface area of face P and Q

The presence of conducting minerals that exist in the soil mass can contribute to lowering the resistance of the soil. Minerals in the soil are either present naturally or added externally to improve the conductivity of the soil. In

certain cases, supplementary minerals such as sodium, calcium, and nitrates are added into the soil if the initial soil resistance is above recommended levels. However, it is worth taking note that in certain cases, the additive minerals may give rise to corrosion of the soil and is undesirable in an environmental sense. Therefore, the addition of conductive minerals into the soil are often carefully evaluated before implementation.

In terms of soil moisture, a moist soil mass tends to have lower resistance as the presence of water in the soil assists in the conduction of current. In practice, the earth electrode is buried at a depth at which the moisture level of the soil is constant throughout. This is because the soil mass that is closer to the surface generally is exposed to uncertain environmental conditions, such as rain and drought affects the level of moisture of the soil to fluctuate. Besides, in case of fault current flowing through the electrode into the earth, the large amount of fault current would generate high levels of heat which would evaporate the moisture of the soil surrounding the electrode.

The level of compactness of the soil also affects the resistance of the soil. Loose soil tends to have higher soil resistance as the soil is more aerated and the path for conduction of fault current is not smooth. Compact soil is generally denser and its resistance is lower as the particles in the soil are closer to each other and therefore conduct electricity better. Factors that would affect the compactness of a soil mass are the presence of rocks or organic materials in the soil that would affect the overall compactness of the soil.

2.4.3.3 Earth Electrode Resistance

The earth electrode that connects the electrical system physically to the earth is not an ideal that is of zero resistance. Generally, as the contact resistance of the earth electrode and the soil mass should be taken into consideration, the resistance of an earth electrode can be determined using the formula

$$R = \frac{\rho}{2\pi L \left[\log \left(\frac{8L}{d} \right) - 1 \right]}$$

Where

R: Resistance of the electrode

ρ : Soil resistivity

L: Length of the electrode

d: Diameter of the electrode

According to IEEE 142, a simplified version of the equation as below is used for a standard earth electrode with a 5/8 inch diameter, driven 10 feet deep into the earth

$$R = \frac{\rho}{3.35}$$

Table 2.1 below is tabulated by IEEE categorizing the soil resistivity and earth electrode resistance with respect to the type of soil mass that is used for earthing.

Table 2.1: Soil and electrode resistance according to soil type (IEEE 142, n.d.)

Soil Type	Average Resistivity (Ω m)	Resistance of Rod Dia. 5/8 in. Length 10 ft in ohms
Well-graded gravel	600–1000	180–300
Poorly graded gravel	1000–2500	300–750
Clayey gravel	200–400	60–120
Silty sand	100–800	30–150
Clayey sands	50–200	15–60
Silty or clayey sand with slight plasticity	30–80	9–24
Fine sandy soil	80–300	24–90
Gravelly clays	20–60	17–18
Inorganic clays of high plasticity	10–55	3–16

2.4.4 Measurements of Earthing System

Soil resistivity plays a major role in the overall earth fault loop impedance. As discussed from the previous subchapter, the resistance of the soil mass used as earthing depends on many factors, one of which is the soil resistivity. Soil resistivity study provides a general understanding of the location and types of earthing system that shall be implemented before the electrical network is built. In large scale construction projects, soil resistivity studies help measure and locate the best position as well as the appropriate type of earth rod to be implemented into the earthing system. A common method to determine the resistivity of a particular soil mass is by applying the 4-pin Wenner Test. The basic setup of a 4-pin Wenner Test is as shown in Figure 2.34.

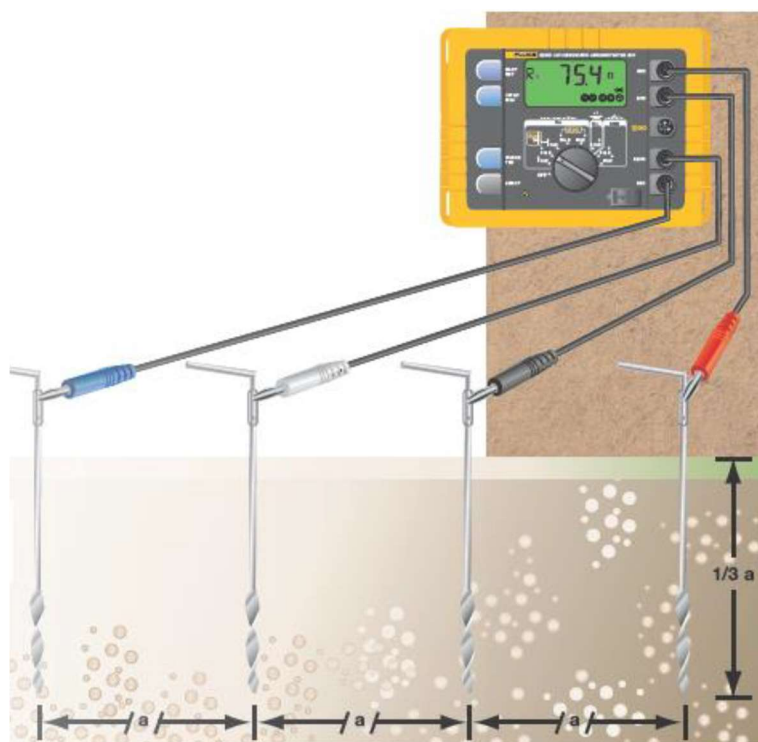


Figure 2.34: Setup for 4-pin Wenner Test (voltimum, 2006)

Describing the functionality of the device shown in Figure 2.34, the device injects current to flow in between the two outer pins (Blue and Red). The voltage drop across the two middle pins (White and Black) is measured by the device and the resistance of the soil mass is calculated and displayed. The depth of which the pins are driven into the earth shall be at least one-third of the spacing between two adjacent pins. For instance, if the depth of the pins is driven 0.5 meters into the earth, the spacing between the pins shall be at least 1.5 meters apart. After obtaining the resistance of the soil mass, the resistivity of the soil is calculated using the equation

$$\rho = 2\pi aR$$

Where

ρ : Average resistivity of the soil

a : Spacing between device pins

R : Resistance of soil

To further improve the accuracy of the readings, the test is performed at multiple locations across the site and the average resistivity is taken as the final reading.

CHAPTER 3

METHODOLOGY AND WORK PLAN

3.1 Introduction

To study the behaviour and characteristic of an SPD in the event of a surge, a surge waveform which fulfils the IEC 61000-4-5 standard shall be first simulated using Simulink provided by MATLAB. Following that, studies on grounding deviation shall be conducted.

3.2 Surge Generator Model

To simulate the implications of surge onto different earth networks, a surge is first required. A simple RLC circuit can be constructed to generate a waveform which is similar to a surge. The RLC circuit must be able to produce a waveform which fulfils the criteria of a surge as defined in the IEC 61000-4-5 standard whereby the overvoltage surge follows a $1.2/50 \mu\text{s}$ waveform, whereas the overcurrent surge shall follow an $8/20 \mu\text{s}$. The RLC circuit which can generate such waveforms simultaneously can be built using Simulink and is shown in Figure 3.1.

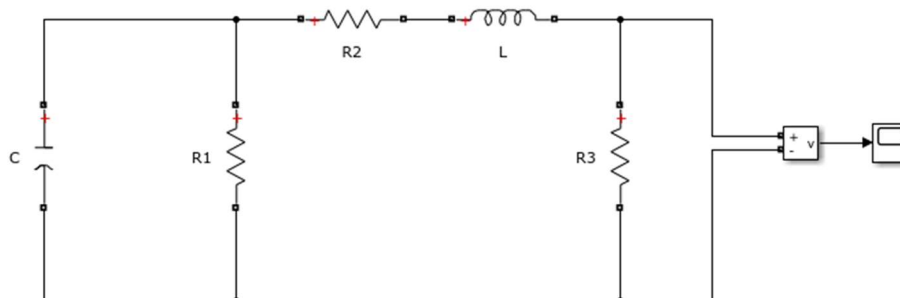


Figure 3.1: Surge generator model

3.3 Network Model

The network model is the electrical network of which the surge will be applied onto it. The network would consist of a source providing power to a load with cables connecting in between. To reduce the complexity of the experiment, a purely resistive load is chosen as a priority instead of an RLC load.

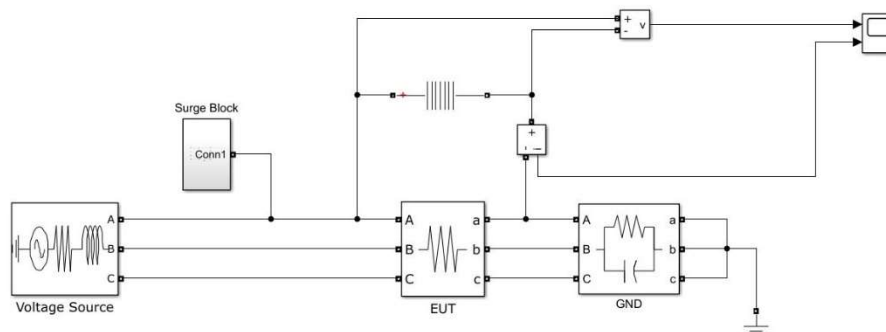


Figure 3.2: Network model

From Figure 3.2, the surge generated from the surge generator will be applied onto either one of the connecting lines in between the source and the load to simulate a surge that is propagating through a cable.

3.4 Earthing Impedance

To study the effects of earthing deviation on the SPD, the ground resistance that is connected to the load will be varied to 20, 40, 60, 80 and 100 Ω to simulate different earth resistances.

3.5 SPD

The SPD will be connected in between one of the phase lines and the different system ground impedances to simulate common mode protection. The SPD is used in this study is a MOV surge arrester SPD.

3.6 Parameters of Study

After the network is all set, the parameters of the SPD that will be monitored across different earthing resistances are:

1. Fall Time
2. Reaction Time
3. Clamping Voltage

Besides that, a study will be performed to investigate the effects of a high impedance earth configuration on the SPD later in the following chapter.

CHAPTER 4

RESULTS & DISCUSSION

4.1 Introduction

In this chapter, the outcomes of the project regarding the surge generator model and the performance of the SPD with earth deviations will be discussed. The SPD that will be used for the simulation is a MOV surge arrester.

4.2 Surge Waveforms

Circuit analysis is performed on the proposed surge generator model in Figure 4.1 below to obtain the appropriate surge waveform is as the following.

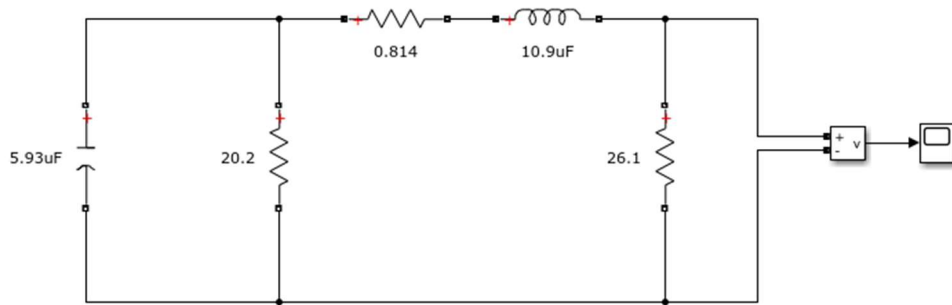


Figure 4.1: Complete surge generator circuit model

Performing circuit analysis, first apply Laplace transform to calculate the output voltage

$$V(s) = \frac{\frac{V_{\text{peak}}}{0.943} \times R_3/L}{s^2 + s \left(R_2 + R_3/L + 1/R_1C \right) + R_1 + R_2 + R_3/R_1LC}$$

The Sum of Roots and Product of Roots of the denominator are

$$\alpha + \beta = \frac{R_2 + R_3}{L} + \frac{1}{R_1C}$$

$$\alpha\beta = \frac{R_1 + R_2 + R_3}{R_1LC}$$

$$V(s) = \frac{\frac{V_{peak}}{0.943} \times R_3/L}{s^2 + s(\alpha + \beta) + \alpha\beta}$$

Applying inverse Laplace to obtain time-domain

$$V(t) = \frac{E \cdot R_3/L}{\beta - \alpha} (e^{-\alpha t} - e^{-\beta t})$$

The time of which the voltage reaches the peak is $t_{peak} = \frac{\ln(\beta/\alpha)}{\beta - \alpha}$

Hence, the equation for the peak voltage is

$$V_{peak} = \frac{E \cdot R_3/L}{\beta - \alpha} (e^{-\alpha t_{peak}} - e^{-\beta t_{peak}})$$

The equation for the current waveform in frequency domain is

$$I(s) = \frac{E/L}{s^2 + s\left(\frac{R_2}{L} + \frac{1}{R_1 C}\right) + \frac{R_1 + R_2}{R_1 LC}}$$

With

$$\omega_0^2 = \frac{R_1 + R_2}{R_1 LC}$$

$$\frac{\omega_0}{Q} = \frac{R_2}{L} + \frac{1}{R_1 C}$$

$$\omega_n = \omega_0 \sqrt{1 - (1/2Q)^2}$$

The simplified equation is

$$I(s) = \frac{E/L}{(s + \omega_0/2Q)^2 + \omega_n^2}$$

In time domain, the current equation becomes

$$I_{\text{peak}} = \frac{E}{\omega_0 L} e^{-\omega_0/2Q t_{\text{peak}}}$$

Where the time of which the current reaches the peak is

$$t_{\text{peak}} = \frac{1}{\omega_n} \tan^{-1}(\sqrt{(2Q)^2 - 1})$$

The elements in the surge generator circuit are calculated using the following equations:

$$C = \left(\frac{1}{R_1} \cdot \frac{\alpha + \beta - \omega_0/Q}{\alpha\beta - \omega_0^2} \right)$$

$$L = \frac{R_3}{\alpha + \beta - \omega_0/Q}$$

$$R_1 = \left(\frac{\omega_0^2}{\alpha\beta - \omega_0^2} \right) \cdot R_3 - R_2$$

$$R_2 = \left(\frac{\omega_0}{Q} - \frac{\alpha\beta - \omega_0^2}{\alpha + \beta - \omega_0/Q} \right) \cdot L$$

$$R_3 = \frac{(\beta - \alpha)e^{-\omega_0/2Q t_{\text{peak}}(\text{current})}}{\omega_0(e^{-\alpha t_{\text{peak}}(\text{voltage})} - e^{-\beta t_{\text{peak}}(\text{voltage})})} \cdot R$$

According to (Carobbi, C.F.M. & Bonci, A., 2013), $\alpha = 0.0147$, $\beta = 2.470$, $Q=1.46$, and $\omega_0=40060\pi$ are substituted into the equations above which eventually gives $C = 5.93 \mu\text{F}$, $L = 10.9 \mu\text{H}$, $R_1 = 20.2 \Omega$, $R_2 = 0.814 \Omega$ and $R_3 = 26.1 \Omega$.

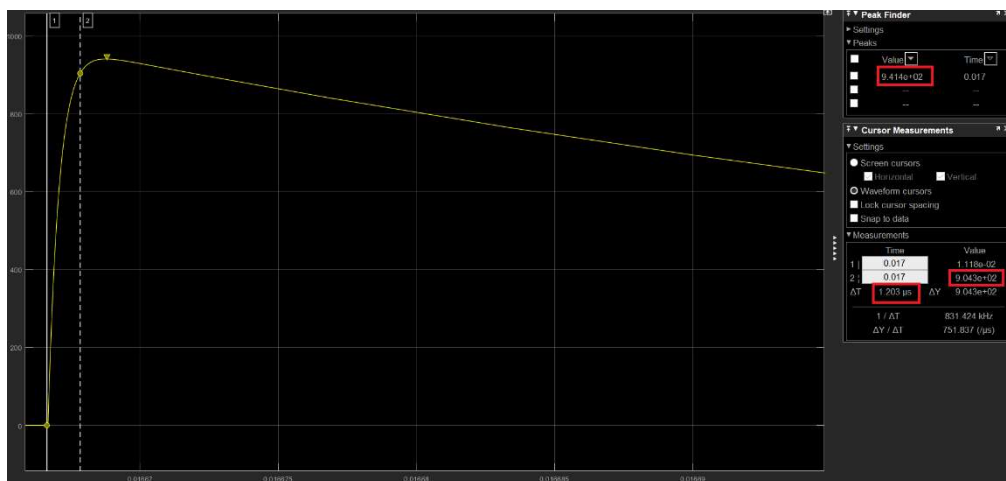


Figure 4.2: Front time of 1.2/50 μs overvoltage surge waveform

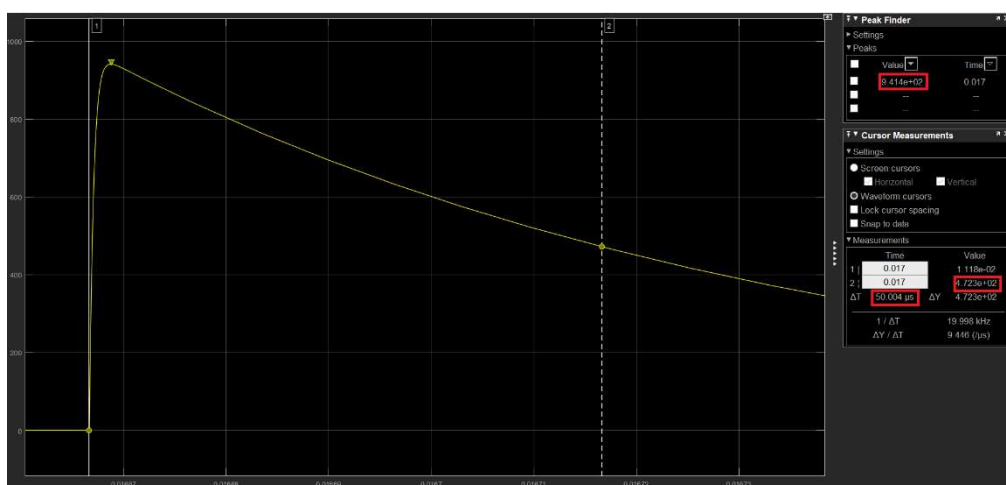


Figure 4.3: Tail time of 1.2/50 μs overvoltage surge waveform

Table 4.1: Comparison table for overvoltage surge

	Theory	Simulated	% Error
Front Time	1.2 μs	1.203 μs	0.25 %
Tail Time	50 μs	50.004 μs	0.008 %

The time taken for the simulated overvoltage waveform to reach its peak value is approximately 1.203 μs while the time taken for it to decay to 50 % of its peak is 50.004 μs as shown in Figure 4.2 and 4.3. By referring to Table 4.1, it can be seen that both the front and tail time of the overvoltage surge waveform is fairly similar to the standard front and tail time as defined by IEC 61000-4-5.

Hence, it can be said that the circuit with the given parameters can fulfil the overvoltage surge waveform standard.

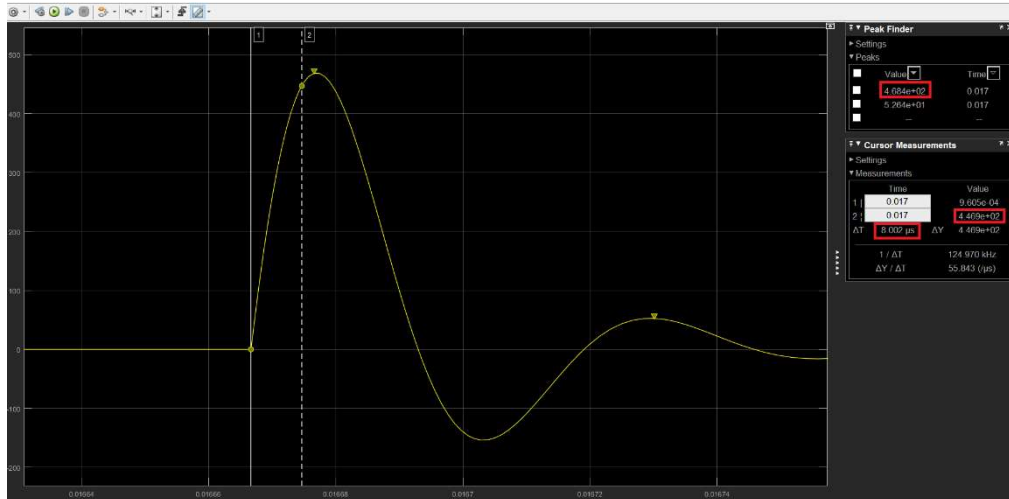


Figure 4.4: Front time of 8/20 μ s overcurrent surge waveform

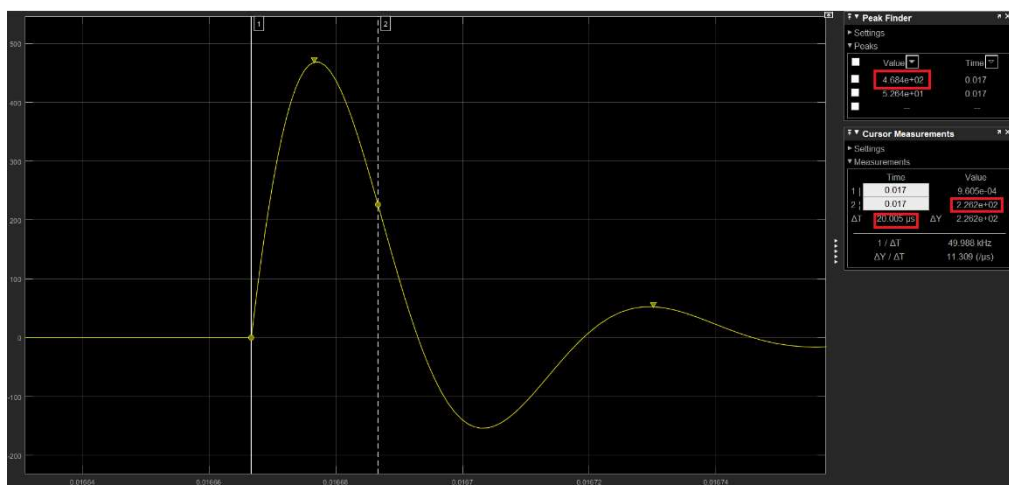


Figure 4.5: Tail time of 8/20 μ s overcurrent surge waveform

Table 4.2: Comparison table for overcurrent surge

	Theory	Simulated	% Error
Front Time	8 μ s	8.002 μ s	0.025 %
Tail Time	20 μ s	20.005 μ s	0.025 %

The time taken for the simulated overcurrent waveform to reach its peak value is approximately $8.002 \mu\text{s}$ while the time taken for it to decay to 50 % of its peak is $20.005 \mu\text{s}$ as shown in Figure 4.4 and 4.5. By referring to Table 4.2, it can be seen that both the front and tail time of the overcurrent surge waveform is fairly similar to the standard front and tail time as defined by IEC 61000-4-5. Hence, it can be said that the circuit with the given parameters can fulfil the overcurrent surge waveform standard.

4.3 MOV Simulation

The surge is applied onto one of the lines connected to the load as shown in Figure 4.6. The voltage waveform of across the load can be seen in Figure 4.7.

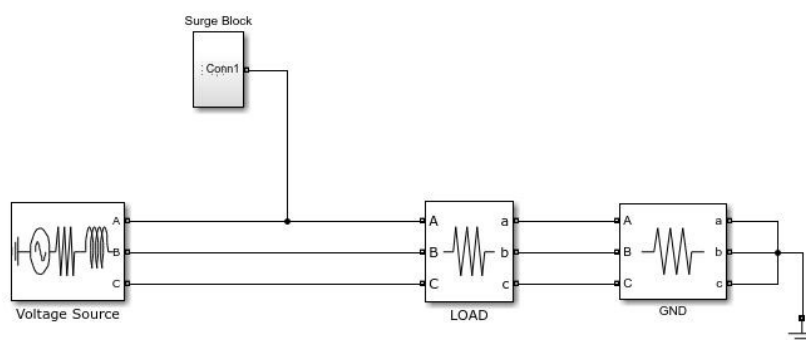


Figure 4.6: Surge applied onto the electrical network

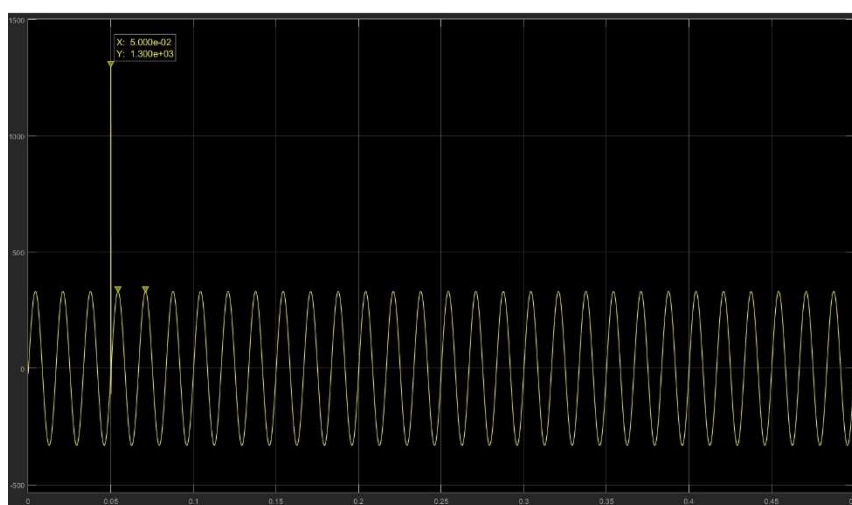


Figure 4.7: Voltage waveform across load

The load voltage is set to $240 V_{\text{rms}}$. When the surge is applied onto the line of the load, a voltage surge peaking at 1.3 kV can be seen on the voltage waveform across the load. As depicted in Figure 4.8, an MOV surge arrester is connected across the load to simulate a common mode protection. The MOV is set to have a clamping voltage of 500 V. The clamping effect of the MOV is shown in Figure 4.9.

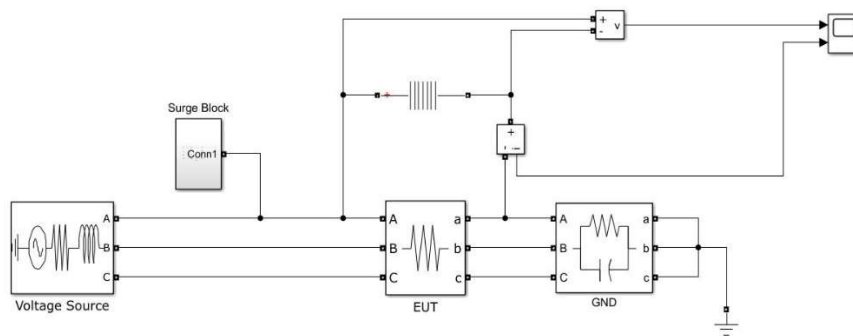


Figure 4.8: MOV connected across load

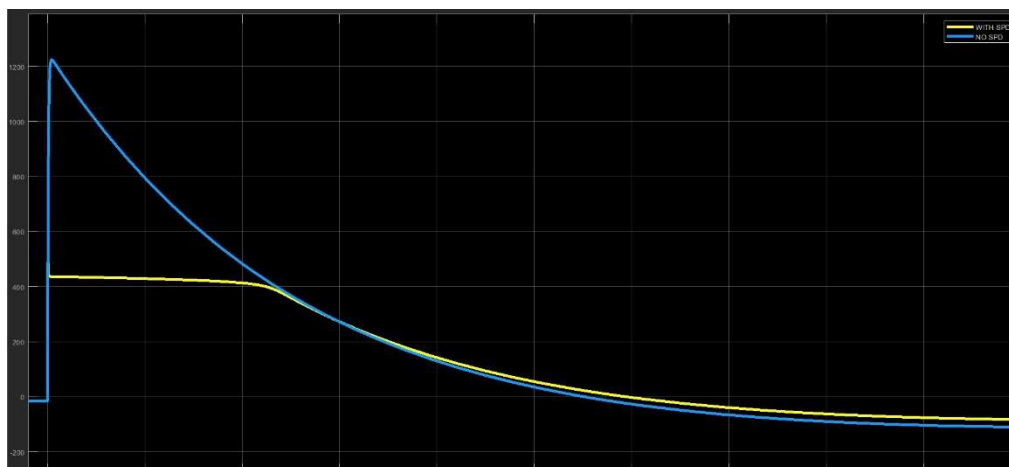


Figure 4.9: Surge waveform with MOV (yellow) & without MOV (blue)

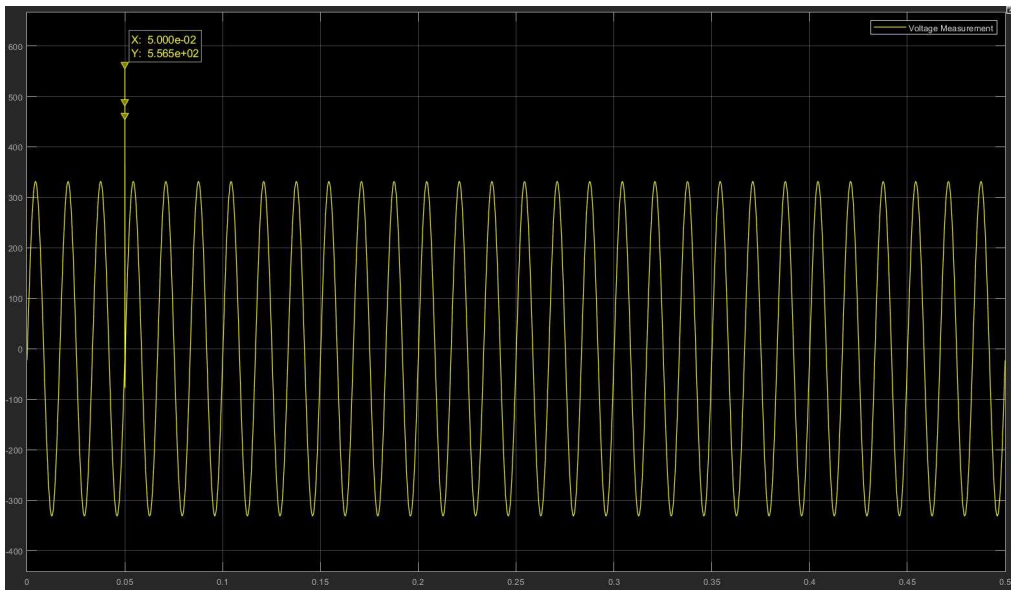


Figure 4.10: Clamped surge voltage

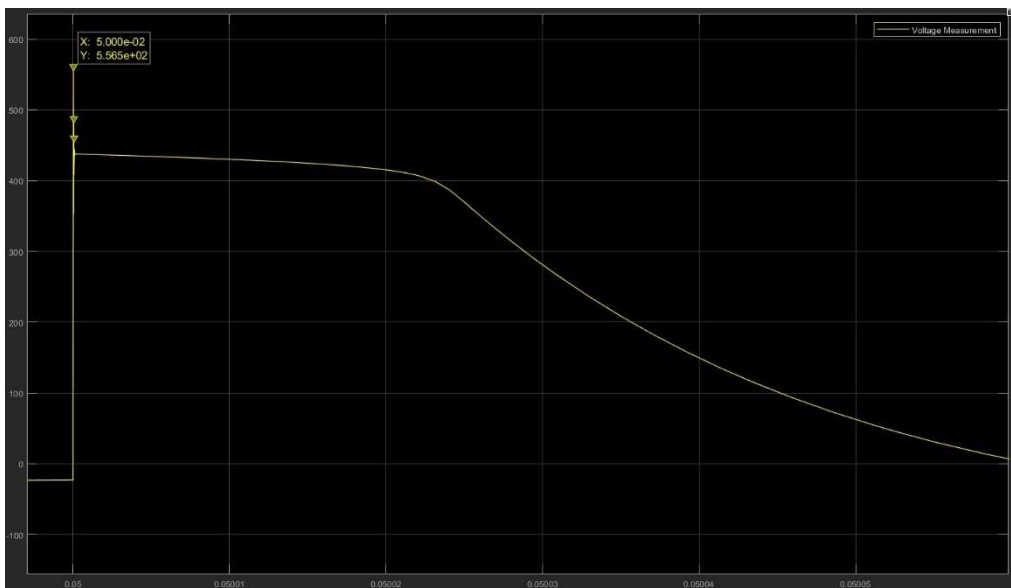


Figure 4.11: Clamped surge voltage (zoomed in)

As seen in Figure 4.9, 4.10, and 4.11, the MOV was able to clamp the surge voltage to a lower level peaking at 556.5 V before falling to a steady state clamping voltage at approximately 446 V. It is worth noting that although the steady state clamping voltage was 446 V instead of the intended 500 V, it is considered that the built-in internal resistance of the MOV has caused this voltage drop to occur.

4.4 MOV Voltage Fall Time

The first parameter to study the performance of the MOV is to determine the fall time of the MOV, that is how fast does the voltage across the MOV falls from the peak clamping voltage to a reference voltage of 400 V. In this section, the ground resistance is varied from 20 Ω to 100 Ω with steps of 20 Ω in between, and the voltage across the MOV for each case is observed using the scope. Figure 4.12 depicts the method that is used to measure the fall time of the MOV.

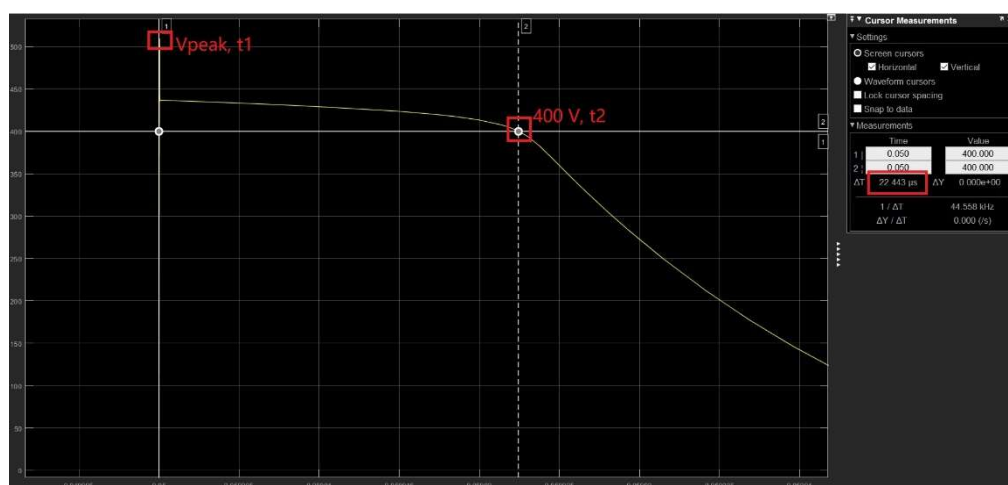


Figure 4.12: Time taken for MOV voltage to drop to 400 V

The formula to calculate the time taken for the MOV to fall to 400 V t_{fall} is

$$t_{\text{fall}} = t_2 - t_1$$

Where

t_1 : time where MOV voltage peaks

t_2 : time where MOV voltage reaches 400 V

The peak clamping voltage and the fall time for the MOV connected to different earth resistance is observed and recorded as shown in Figure 4.13 and Table 4.3 below.

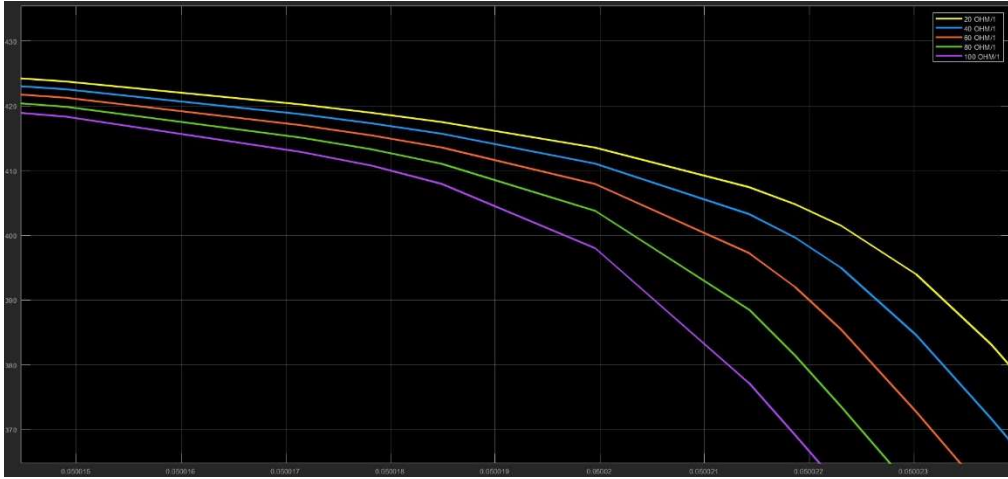


Figure 4.13: MOV voltage falling to 400 V for different earth resistance

Table 4.3: MOV peak voltage and fall time

Earth Resistance (Ω)	MOV Peak Clamping Voltage (V)	t_{fall} (μs)
20	509.6	22.4
40	488.5	21.8
60	474.0	21.1
80	462.3	20.3
100	452.9	19.7

From Figure 4.13 and Table 4.3, it can be seen that the voltage across the MOV that is connected to a higher earth resistance falls faster to 400 V as compared to when it is connected to a lower earth resistance. The results imply that a higher earth impedance is more ideal as it would cause the voltage across the MOV to return to normal operating levels quicker. This contradicting result can be justified as the network itself acts like a potential divider circuit, whereby having a higher ground resistance would result in a lower voltage drop across the MOV; thus, resulting in a faster fall rate. The relationship of the voltage across the MOV and the ground resistance can be expressed as

$$V_{\text{mov}} = \frac{R_{\text{MOV}}}{R_{\text{MOV}} + R_{\text{earth}}} \times V_{\text{surge}}$$

$$\therefore V_{\text{mov}} \propto \frac{1}{R_{\text{earth}}}$$

The relationship above shows that the MOV voltage is inversely proportional to the earth resistance. This hypothesis is further verified by measuring the voltage across the MOV and ground resistor using Simulink. Table 4.4 below shows the potential across the MOV and the earth resistance at the same instance. The measurements are considered consistent as the sum of voltage across the MOV (V_{mov}) and the earth resistance (V_{earth}) equals to the surge peak voltage of 1.3 kV for every case.

Table 4.4: MOV voltage vs potential across earth resistance

MOV Voltage (V)	Earth Resistance Voltage (V)
509.6	790.4
488.5	811.5
474.0	826.0
462.3	837.7
452.9	847.1

Hence, it can be concluded that having a higher earth resistance would reflect to a lower potential drop across the MOV, which in turn leads to a faster fall rate.

4.5 MOV Reaction Time

The MOV response time measures how fast does the MOV start clamping the surge voltage at different earth resistances. The method to measure the reaction of the MOV is by measuring the time taken of the turning point of the peak voltage across the MOV as depicted in Figure 4.14 below.



Figure 4.14: Time taken for MOV to react towards surge

To calculate the reaction time of the MOV, the equation used is

$$t_{\text{react}} = t_2 - t_1$$

Since the surge is set to be applied at 0.5 s, $t_1 = 0.5$ s. t_2 is observed using a scope and the results are recorded as below in Table 4.5.

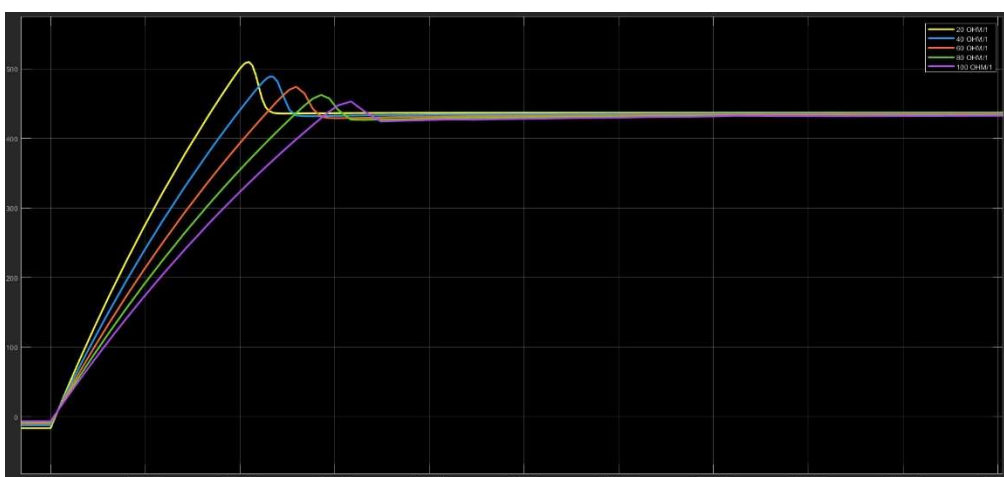


Figure 4.15: Reaction time of MOV for different earth resistances

Table 4.5: Reaction time of MOV for different earth resistances

Earth Resistance (Ω)	MOV Peak Clamping Voltage (V)	Reaction Time (μ s)
20	509.6	41.9
40	488.5	47.0
60	474.0	51.9
80	462.3	57.2
100	452.9	63.4

From the Figure 4.15, it can be seen that the MOV which is connected to the lowest earth resistance (20 Ω) achieves peak the fastest while the one connected to largest earth resistance (100 Ω) is the last. Table 4.5 shows that the MOV that is connected to a lower earth resistance reacts the fastest towards clamping surges. This agrees with the fact that a lower earth resistance is more desirable in practical applications.

As discussed in the previous section, for a lower earth resistance, the peak voltage across the MOV is higher and this would cause the MOV to react more aggressively to clamp the surge. Thus, it can be concluded that the MOV reacts faster when it is connected to a lower earth impedance.

4.6 MOV Clamping Voltage

In the simulation, the MOV is set to have a clamping voltage of 500 V. This means that the MOV will activate once the voltage across the MOV exceeds 500 V. As there will be a certain amount of overshoot voltage across the MOV at the instance when the surge is applied, the clamping voltage of the MOV is measured once the MOV clamping voltage achieves steady state. Figure 4.16 shows the overshoot voltage and the steady state clamping voltage of the MOV.



Figure 4.16: Steady state clamping voltage of MOV

The steady state clamping voltage of the MOV for different earth resistances at the same instance is as shown in Figure 4.17 and is recorded in Table 4.6.

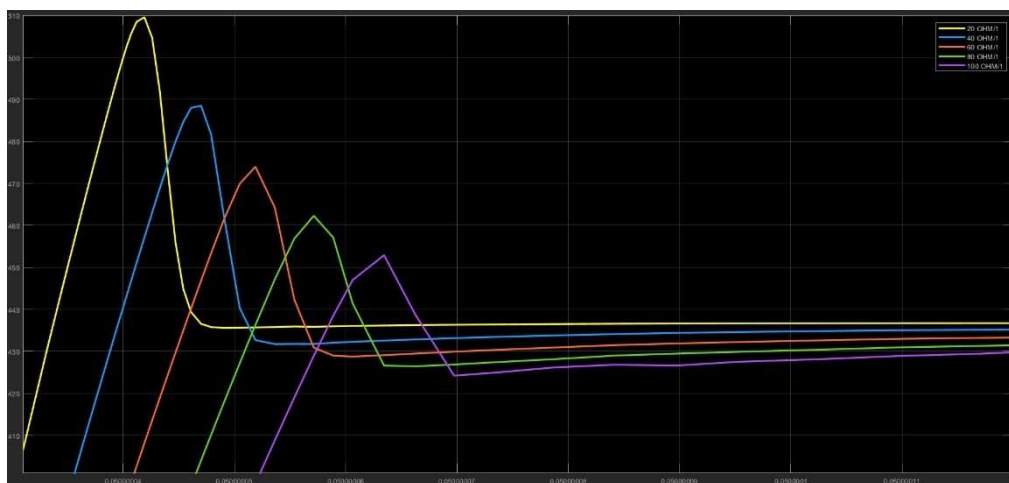


Figure 4.17: Steady state clamping voltage of MOV for different earth resistance

Table 4.6: Steady state clamping voltage of MOV

Earth Resistance (Ω)	MOV Steady State Clamping Voltage (V)
20	437
40	435
60	432
80	430
100	428

From the results obtained in Table 4.6, the clamping voltage of the MOV which is connected to a higher earth resistance is lower compared to one that is connected to a higher earth resistance. This result further justifies the potential divider hypothesis as stated in **section 4.4** where it was shown that a higher earth resistance would cause a lower potential difference to reflect across the MOV. Thus, in the case of clamping voltage of the MOV, a higher earth resistance is more desirable.

4.7 High Impedance Earth

To study the effects of a high impedance earth on the MOV, the earth resistance is configured to $1\text{ M}\Omega$ while the load in the simulation is set to only $100\ \Omega$. This is sufficient to simulate a high earth impedance as relative to the load, the earth resistance is 10,000 times higher. The network is configured as shown in below in Figure 4.18.

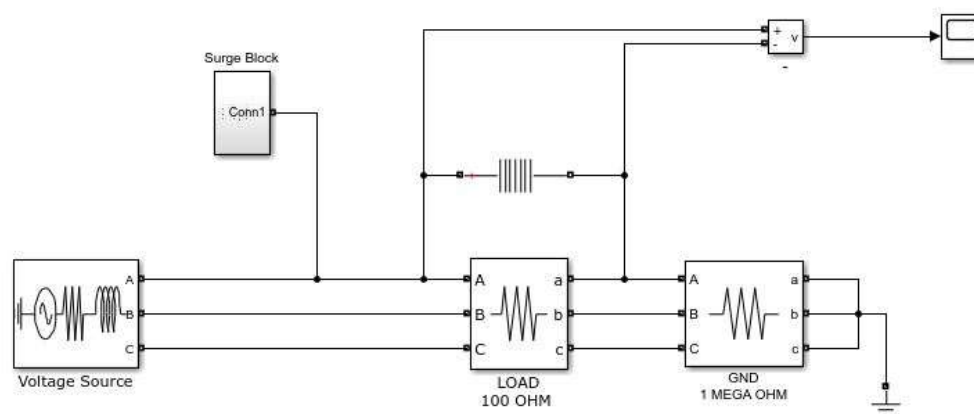


Figure 4.18: High impedance earth network

Figure 4.19 shows the voltage waveform across the MOV when the surge is applied onto the network. As reference, the waveform of a MOV that is connected to a $20\ \Omega$ ground resistance is plotted on the same figure for comparison purposes.

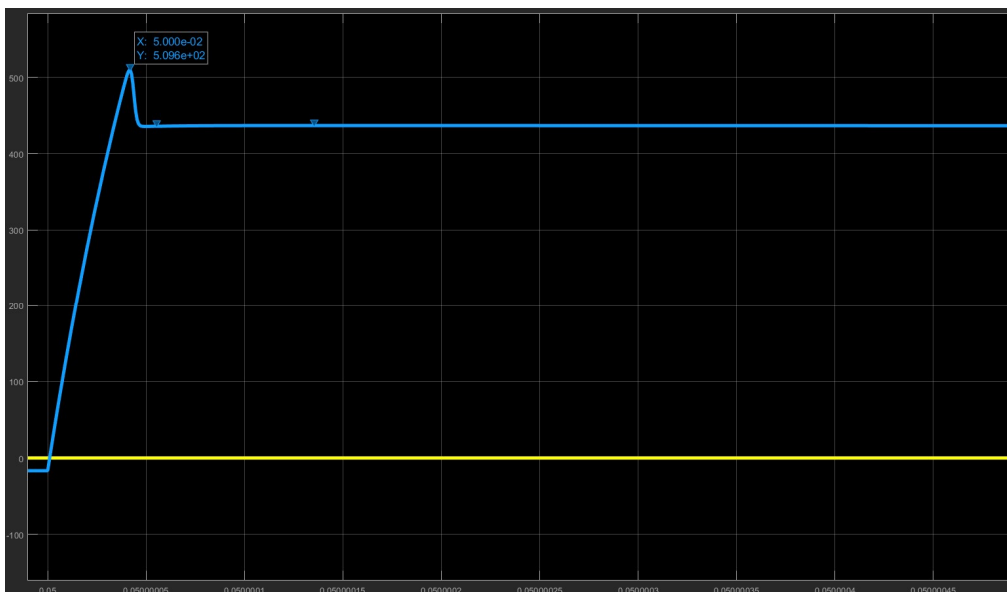


Figure 4.19: Voltage waveform of MOV with 20 Ω earth resistor (blue) vs 1 $M\Omega$ earth resistor (yellow)

From the figure above, it is observed that the MOV connected to the 1 $M\Omega$ earth resistance does not show any sign of voltage across it. From the previous potential divider hypothesis, this implies that all the surge voltage has been reflected onto the high earth resistance instead of the MOV itself, resulting in a zero voltage drop across the MOV. Figure 4.20 shows the voltage across the MOV and the 1 $M\Omega$ earth resistance when the surge is applied.

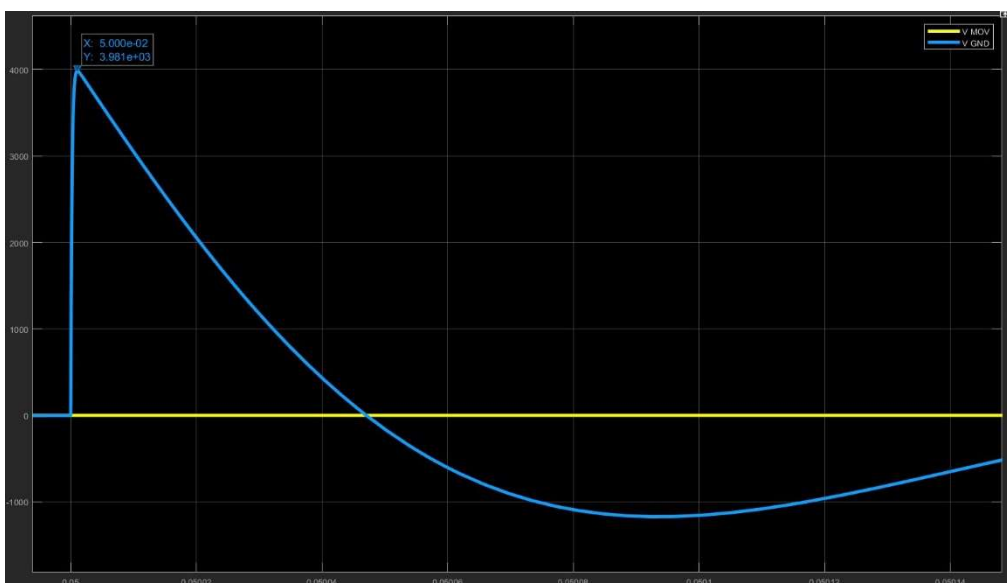


Figure 4.20: Voltage waveform of earth resistor (blue) vs voltage across MOV (yellow)

When a 1 k Ω earth resistance is configured to further experiment on this factor, the voltage across the MOV reaches a peak of only 30.5 V as shown in Figure 4.21, which is not high enough to trigger the MOV to turn on and operate as the voltage reference of the MOV is set at 500 V.

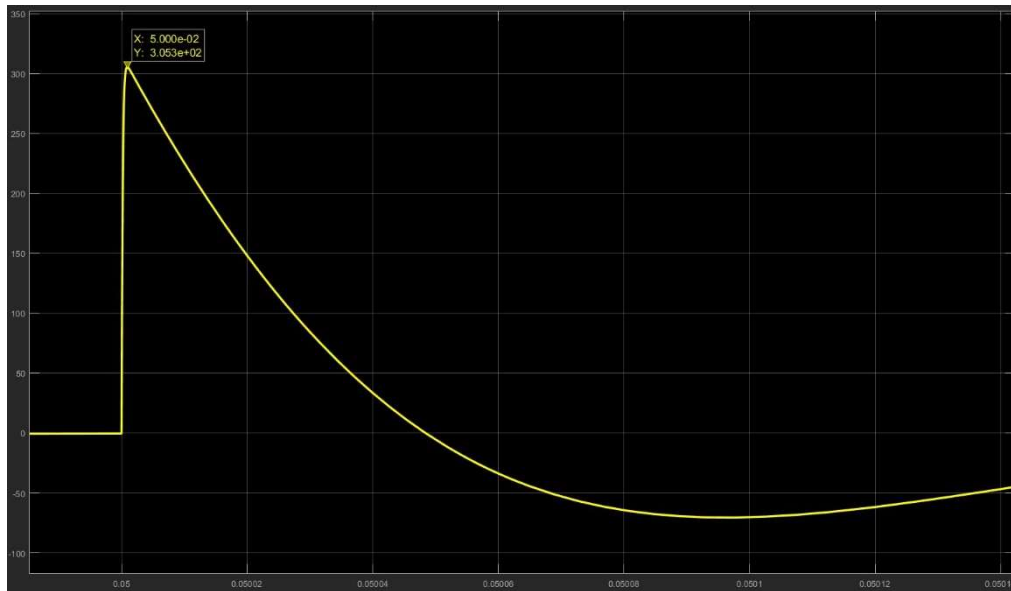


Figure 4.21: MOV voltage waveform with 1000 Ω earth resistance

This result proves that when a high earth resistance is applied relative to the load, the MOV cannot operate as the voltage across the MOV would not be higher than its reference voltage for it to turn it on. Therefore, from this simulation, it is recommended that the earth resistance shall not exceed the resistance of the load as this would cause complications in terms of activating the MOV to operate and clamp the surge.

CHAPTER 5

CONCLUSION AND RECOMMENDATIONS

5.1 Conclusion

The main objective of this project is to investigate the effects of earthing on the performance of the SPD besides understanding the nature of power surges.

It was studied that electrical surges can be of either internally or externally introduced into a system. External sources of surges include lightning strikes while load switching causes surges within the system. A surge generator model was designed using MATLAB Simulink and it was able to generate a surge waveform that fulfils IEC 61000-4-5. The surge was applied onto an electrical network which includes a MOV surge arrester as protection connected to a varying earth resistance to simulate different earthing conditions.

As far as how the voltage characteristic of the MOV respond towards different earth resistances, it was shown that having a higher earth resistance would cause the voltage across the MOV to be lower. This contradicts with the idea of a high earth impedance is less efficient as the results has shown otherwise. The hypothesis of a potential divider circuit was used to verify the results and the hypothesis shows consistency throughout different experiments.

For the reaction time of the MOV towards the surge when connected to different earth resistances, a higher earth resistance contributed to a slower reaction. This was mainly caused by the lower potential drop reflected across the MOV, resulting in a less aggressive reaction from the MOV.

In conclusion, in terms of protecting an equipment from overvoltage conditions due to surges, a higher earth impedance seems to show more promising results than lower earth impedance. However, it is worth noting that this project mainly focuses on the voltage aspect of the network. Having a high earth impedance would cause complications in terms of efficiently diverting the surge current. Further research regarding achieving balance in between protecting equipment from overvoltage and overcurrent conditions is required.

5.2 Recommendations

As the SPD used in this research is a clamping type MOV surge arrester, the parameters that were studied surrounds the voltage aspect of the SPD rather than a more comprehensive study which includes the current characteristic. Further studies can include verifying the potential divider hypothesis and the current characteristic of an SPD during surge conditions.

REFERENCES

- Carobbi, C.F.M. and Bonci, A., 2013. Elementary and ideal equivalent circuit model of the 1,2/50 - 8/20 μ s combination wave generator. *IEEE Electromagnetic Compatibility Magazine*, 2(4), pp.51–57.
- Continuous, M., Voltage, V. and Peak, M., 2011. MOV-14DxxxK Series - Metal Oxide Varistor Electrical Characteristics (@ T A = 25 ° C Unless Otherwise Noted) SMD - Trimming Potentiometer.
- Fotis, G.P., Gonos, I.F. and Stathopoulos, I.A., 2004. Simulation and experiment for surge immunity according to EN 61000-4-5. *Series on Energy and Power Systems*, pp.647–652.
- Gomes, C., 2011. On the selection and installation of surge protection devices in a TT wiring system for equipment and human safety. *Safety Science*, [online] 49(6), pp.861–870. Available at: <<https://dx.doi.org/10.1016/j.ssci.2011.02.002>>.
- IAS, 2007. IEEE Recommended Practice for Grounding of Industrial and Commercial Power Systems - Redline. *IEEE Std 142-2007 (Revision of IEEE Std 142-1991) - Redline*, 2007, pp.1–215.
- Kawamura, T., Harada, I. and Matsushita, T., 1991. Lightning surge protector. [online] Available at: <<https://patents.google.com/patent/US5191503A/en?q=US5191503A>>.
- Lacroix, B. and Calvas, R., 2011. Cahier technique no. 172 System earthings in LV. *Gui*, 19(83), pp.1–13.
- Sheeba, R., Jayaraju, M. and Shanavas, T.K.N., 2012. Simulation of impulse voltage generator and impulse testing of insulator using MATLAB simulink. *World Journal of Modelling and Simulation*, 8(4), pp.302–309.
- STMicroelectronics, 2013. Application note: IEC 61000-4-5 standard overview. *Www.St.Com*, (August 2013), pp.1–11.
- Uman, M.A., 2008. *The art and science of lightning protection. The Art and Science of Lightning Protection*.
- Verma, V.K., 2014. Practical Simulation and Modelling of Lightning Impulse Voltage Generator using Marx Circuit. (November), pp.9–11.

APPENDICES

Appendix A: IEEE C62.41.2 STANDARD

IEEE Std C62.41.2™-2002

IEEE Standards

C62.41.2™**IEEE Recommended Practice on
Characterization of Surges in
Low-Voltage (1000 V and Less)
AC Power Circuits****IEEE Power Engineering Society**Sponsored by the
Surge Protective Devices CommitteePublished by
The Institute of Electrical and Electronics Engineers, Inc.
3 Park Avenue, New York, NY 10016-5997, USA

11 April 2003

Print: SH95031
PDF: S095031

Recognized as an
American National Standard (ANSI)

IEEE Std C62.41.2™-2002

IEEE Recommended Practice on Characterization of Surges in Low-Voltage (1000 V and Less) AC Power Circuits

Sponsor

**Surge Protective Devices Committee
of the
Power Engineering Society**

Approved 10 March 2003

American National Standards Institute

Approved 11 November 2002

IEEE-SA Standards Board

ports, but by understanding the *interaction* scenario and providing effective remedial measures to address that stress. Consensus has not yet been reached on what representative waves and values should be recommended for that mechanism; therefore, this recommended practice does not include these waves and values in its scope.

4.5 Location categories—Scenario I

As a first step toward a reduction of the complex database on surge occurrences for Scenario I, the concept of location categories is proposed here. Figure 2 shows a pictorial description, including the transitions provided by the physical characteristics and components of the power system. Table 1 presents recommendations on the applicable representative waveforms, and Table 2 through Table 7 present stress levels that might be expected in each category. *As emphasized repeatedly in this recommended practice, this process remains a simplified description of the environment, not an equipment specification.*

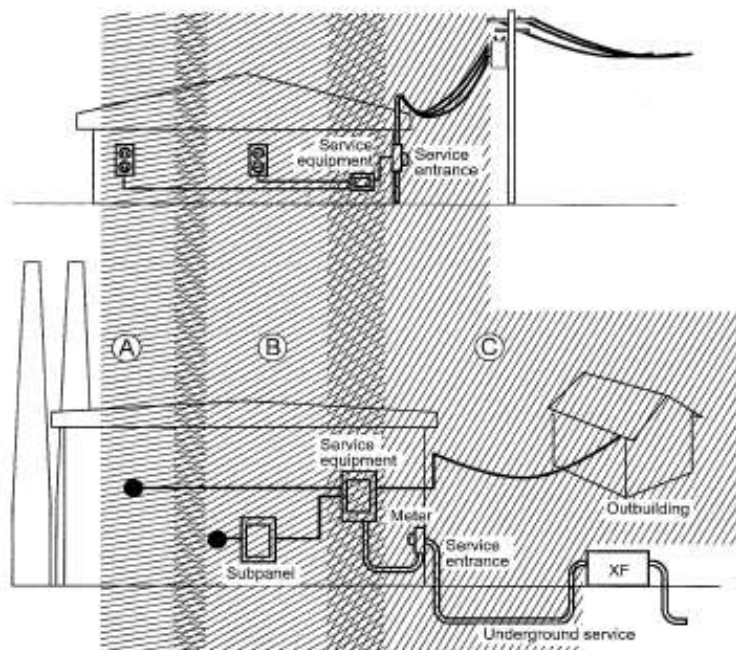
According to this concept, Location Category A applies to the parts of the installation at some distance from the service entrance. Location Category C applies to the external part of the structure, extending some distance into the building. Location Category B extends between Location Categories C and A. Because the reality of surge propagation is clearly a continuous situation, separating the categories by sharp conceptual boundaries would be an arbitrary and debatable process. Instead, the concept of location categories recognizes the existence of transition bands that connect the categories by overlapping. These transitions can be associated with the presence of an identifiable device or component: a clearance can provide a limiting of voltage by flashover; and a surge current can be reduced by diversion through an SPD or impeded by the impedance of the wiring.

The concept of location category rests on the considerations discussed in 5.2 and 5.3 in IEEE Std C62.41.1-2002 on dispersion and propagation of surge currents and surge voltages. For surge currents presented at the service entrance of a building, the increasing impedance opposing (impeding) the flow of surge currents further into the building—with or without the crowbar effect of flashover at the service entrance—reduces the surge current that can be delivered along the branch circuits (Mansoor and Martzloff 1997 [B23]). In contrast, a voltage surge presented at the service entrance of a building (unless limited by clearance flashover) can propagate, practically unattenuated, to the end of a branch circuit when no low-impedance load (equipment or local SPD) is present there (Martzloff 1983 [B25]; 1986 [B26]; 1990 [B27]; 1991 [B28]).

In Figure 2, Location Categories A, B, and C correspond to the scenario of surges impinging on the service entrance or generated within the building. A direct flash to the structure produces by induction voltage and current surges in the circuits of the building. However, such induced surges occur during the initial rise of the lightning current and, therefore, can be represented by relatively short-duration surges involving relatively low energy deposition capability, such as the 100 kHz Ring Wave. The resistively coupled surges resulting from a direct flash (Scenario II) involve long tails, so that their dispersion is not affected by the wiring inductance after the initial part of the surge, which is the significant parameter in the location category concept.

4.6 Direct flash to the structure—Scenario II

Scenario II has been proposed to describe the special case of a direct flash to the structure or of a flash to earth very close to the structure. Significant factors include the flash density for the area of concern, the effective collection area of the structure, the statistical distribution of peak amplitudes, the relationship between first stroke and subsequent strokes, and the dispersion of the lightning current in the available paths to ground. There are two related phenomena occurring with a direct strike to the facility. One effect is the induction of surges into the surrounding circuits by the high electromagnetic field produced by the high-current, fast-rising lightning flash. The resulting surges can be represented by a Ring Wave, as described in 6.3.1. The other effect is the direct injection of current into the ground system. Briefly summarized here, it is discussed in more detail in 5.5 of IEEE Std C62.41.1-2002. In that subclause, data are given on flash density



NOTE—There can be differences in the configuration and distance between the revenue meter and the service equipment. This schematic is only an example to illustrate the concept of location categories. [The National Electrical Code® (NEC®) (NFPA 70-2002) [B32] states in Article 230-70 “The service disconnecting means shall be installed at a readily accessible location either outside of a building or structure, or inside nearest point of entrance of the service conductors.”]

Figure 2—The concept of location categories and transitions as simplification approach

maps, and in C.7 of IEEE Std C62.41.1-2002 an example is given of computation of the average annual frequency of direct flashes to a specified structure. Indeed, an important aspect of Scenario II is its low probability of occurrence for a particular building, although lightning flashes are globally frequent events. In the case of a flash to earth very close to the structure, a significant part of the current can disperse directly into the soil, while the remainder is likely to flow into the earthing system of the structure, as if injected by a direct flash, but with some reduction of the amplitude. Therefore, a specific risk analysis, taking in consideration the function of the building, should be performed before discounting or mandating the need for adequate surge protection in this rare scenario for one specific installation.

The lightning current parameters defined in IEC publications are based on the results of Study Committee 33 of CIGRE (International Conference on Large High Voltage Electric Systems) (Berger et al. 1975 [B5]; Anderson and Eriksson 1980 [B1]). *Note that these studies characterized the lightning flash itself, not the resulting lightning surges in the ac power circuits of the struck building.*

Criteria for selection of the peak voltages and currents that correspond to various environmental exposures are discussed in 6.2 with reference to Table 2 through Table 5. A more detailed description of these two standard waveforms is given in 6.3. Tolerances to be applied for testing and equations describing the waveforms that might be used in numerical simulations are given in IEEE Std C62.45-2002. For SPD testing applicable to the Category C environment, two separate surge generators may be used to perform respectively a current test and a voltage test.

6.1.1 The 100 kHz Ring Wave

A plot of the nominal Ring Wave is shown in Figure 4, and further details are given in 6.3.1. No short-circuit current waveform is specified for the 100 kHz Ring Wave. A peak short-circuit current amplitude, however, is proposed in 6.2, according to the location category. The nominal ratio of peak open-circuit voltage to peak short-circuit current (effective impedance) is specified to be $12\ \Omega$ for simulation of Location Category B environments or $30\ \Omega$ for simulation of Location Category A environments. The nominal amplitude of the first peak is selected by the parties involved (see 6.2), according to the severity desired.

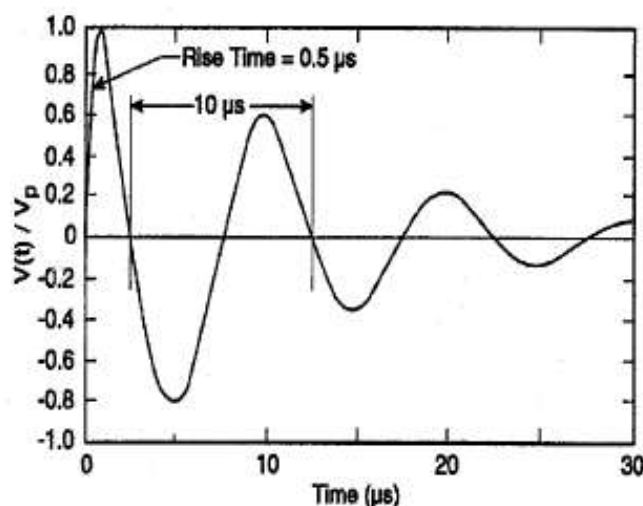


Figure 4—The 100 kHz Ring Wave (voltage and current)

6.1.2 The Combination Wave

The Combination Wave involves two waveforms, an open-circuit voltage and a short-circuit current, shown in Figure 5 and Figure 6, respectively. Further details are given in 6.3.2. The Combination Wave is delivered by a generator that applies a $1.2/50\ \mu\text{s}$ voltage wave across an open circuit and an $8/20\ \mu\text{s}$ current wave into a short circuit. The exact waveform that is delivered is determined by the generator and the impedance of the equipment under test (EUT) to which the surge is applied. The value of either the peak open-circuit voltage or the peak short-circuit current is to be selected by the parties involved (see 6.2), according to the severity desired.

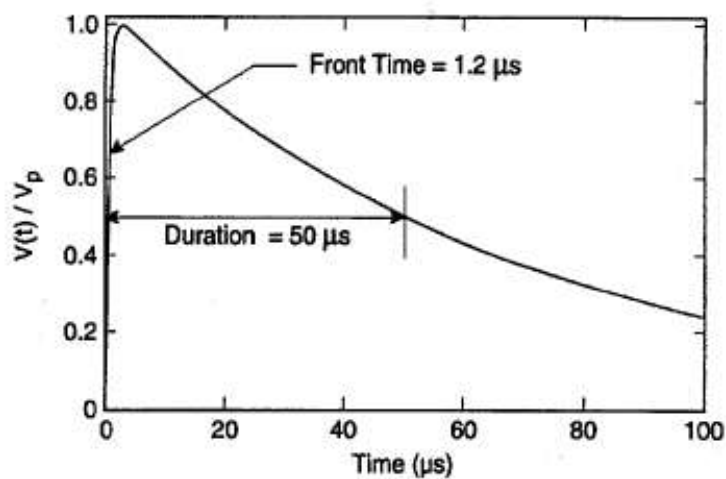


Figure 5—Combination Wave open-circuit voltage

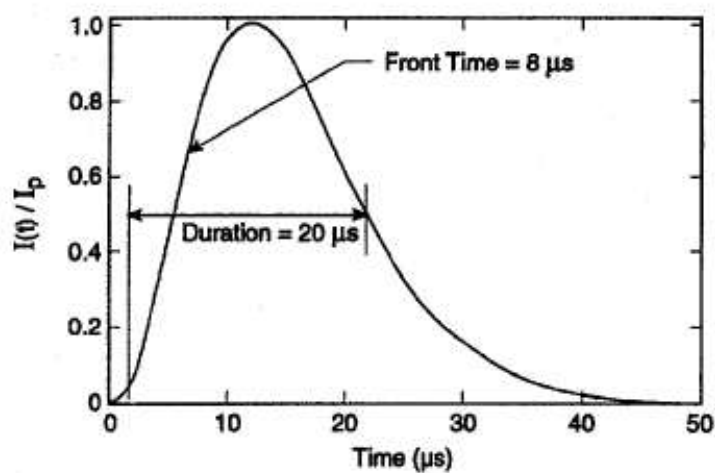


Figure 6—Combination Wave short-circuit current

6.2 Selection of peak values of standard waveforms

Table 2 through Table 5 include a matrix of location categories, types of surges, peak voltages, and peak currents provided as a guide toward the selection of an appropriate set of design parameters or tests. It is emphasized that these parameters in the matrix can only provide a menu. *They are not intended to be mandatory requirements.*

Table 2—Standard 0.5 μ s–100 kHz Ring Wave
Expected maximum voltage and current surges in Location Categories^a A and B^b
Single-phase modes^c: L-N, L-G, and [L&N]-G
Polyphase modes: L-L, L-G, and [L's]-G
 (See Table 5 for N-G mode)

Location Category ^a	Peak values ^d		Effective impedance (Ω) ^e
	Voltage (kV)	Current (kA)	
A	6	0.2	30
B	6	0.5	12

^aSee 4.5 for definition and discussion of location categories.

^bA 100 kHz Ring Wave may be optional in Category C when front-of-wave response is a concern.

^cSee IEEE Std C62.45-2002 for discussion of coupling modes.

^dThe values shown for Location Categories A and B have been set by consensus to provide guidance and uniformity in test procedures and in SPD selection. Other levels may be negotiated between the parties involved, including the particulars of a situation where the transitions between categories can be specifically assessed.

^eThe effective impedance of the surge source (emulated by a test generator) is defined as the ratio of the peak voltage to the peak current. It has the dimension of a resistance, but it is not a pure resistance (see 6.3.1).

Table 3—Standard 1.2/50 μ s–8/20 μ s Combination Wave
Expected voltages and current surges in Location Categories^a A and B^b
Single-phase modes^c: L-N, L-G, and [L&N]-G
Polyphase modes: L-L, L-N, L-G, and [L's]-G
 (See Table 5 for N-G modes)

Location Category ^a	Peak values ^d		Effective impedance (Ω) ^e
	Voltage (kV)	Current (kA)	
A	6	0.5	12 ^f
B	6	3	2

^aSee 4.5 for definition and discussion of location categories.

^bSee Table 4 for Combination Wave application to a low exposure in Location Category C.

^cSee IEEE Std C62.45-2002 for discussion of coupling modes.

^dThe values shown for each location category have been set by consensus to provide guidance and uniformity in test procedures. Other levels may be negotiated between the parties involved, including the particulars of a situation where the transitions between categories can be specifically assessed.

^eThe effective impedance of the surge source (emulated by a test generator) is defined as the ratio of the peak voltage to the peak current. It has the dimension of a resistance, but is not a pure resistance (see 6.3.2).

^fNominally, a 12 Ω effective impedance. To allow using a surge generator with 2 Ω impedance, a 10 Ω non-inductive resistor may be added, recognizing that the waveform might be slightly changed.

The short 0.5 μs rise time of the leading edge of the waveform, together with a large peak current, corresponds to a large value of di/dt , which will produce significant inductive effects in the connections of the devices under test. The voltage divider action of the surge generator impedance and the EUT impedance is likely to be significant; it is addressed by specifying the peak short-circuit current.

The 1980 edition of this document (IEEE Std 587) specified a nominal rate of decay of amplitude of 60% between adjacent peaks of opposite polarity, but no tolerances were specified. When tolerances were added, large tolerances were applied to the ratio of the first and second peaks so that a cosine waveform with an exponentially decaying amplitude would meet the requirements for the Ring Wave. Although existing generators are acceptable, it is recommended that new designs for 100 kHz Ring Wave generators use the damped cosine waveform defined by the equations given in IEEE Std C62.45-2002.

The frequency of oscillation of this waveform may excite resonances in the EUT. However, this effect cannot be positively identified with the fixed-frequency Ring Wave; a swept-frequency test would be necessary for that purpose.

6.3.2 The 1.2/50 μs –8/20 μs Combination Wave

The Combination Wave is delivered by a generator that can apply a 1.2/50 μs voltage wave across an open circuit and an 8/20 μs current wave into a short circuit. The exact waveform that is delivered is determined by the generator and the impedance of the EUT and its connections to which the surge is applied. A plot of the nominal open-circuit voltage has been shown in Figure 5, and a plot of the nominal short-circuit current has been shown in Figure 6.

6.3.2.1 Open-circuit voltage waveform

- Front time: 1.2 μs
- Duration: 50 μs

The front time for voltage waveforms is defined (IEC 60060-2:1994 [B12]; IEEE Std 4[™]-1995 [B21]) as

$$1.67 \times (t_{90} - t_{30})$$

where

t_{90} and t_{30} are the times of the 90% and 30% amplitudes on the leading edge of the waveform.

The duration is defined as the time between virtual origin and the 50% amplitude point on the tail.

The virtual origin is the point where a straight line between the 30% and 90% points on the leading edge of the waveform intersects the $V = 0$ line.

6.3.2.2 Short-circuit current waveform

- Front time: 8 μs
- Duration: 20 μs

The front time for current waveforms is defined (IEC 60060-2:1994 [B12]; IEEE Std 4-1995 [B21]) as

$$1.25 \times (t_{90} - t_{10})$$

where

t_{90} and t_{10} are the times of the 90% and 10% points on the leading edge of the waveform.